applied sciences

MDPI

Article

The MINLP Approach to Topology, Shape and Discrete Sizing Optimization of Trusses

Simon Šilih [1,*], Zdravko Kravanja [2] and Stojan Kravanja [3]

[1] ANDRITZ AG, Stattegger Strasse 18, 8045 Graz, Austria
[2] Faculty of Chemistry and Chemical Engineering, University of Maribor, Smetanova 17, 2000 Maribor, Slovenia; zdravko.kravanja@um.si
[3] Faculty of Civil Engineering, Transportation Engineering and Architecture, University of Maribor, Smetanova 17, 2000 Maribor, Slovenia; stojan.kravanja@um.si
* Correspondence: simon.silih@gmail.com

Abstract: The paper presents the Mixed-Integer Non-linear Programming (MINLP) approach to the synthesis of trusses. The solution of continuous/discrete non-convex and non-linear optimization problems is discussed with respect to the simultaneous topology, shape and discrete sizing optimization of trusses. A truss MINLP superstructure of different topology and design alternatives has been generated, and a special MINLP model formulation for trusses has been developed. In the optimization model, a mass objective function of the structure has been defined and subjected to design, load and dimensioning constraints. The MINLP problems are solved using the Modified Outer-Approximation/Equality-Relaxation (OA/ER) algorithm. Multi-level MINLP strategies are introduced to accelerate the convergence of the algorithm. The Modified Two-Phase and the Sequential Two-Phase MINLP strategies are proposed in order to solve highly combinatorial topology, shape and discrete sizing optimization problems. The importance of local buckling constraints on topology optimization is also discussed. Some simple numerical examples are shown at the end of the paper to demonstrate the suitability and efficiency of the proposed method.

Keywords: structural synthesis; topology optimization; discrete sizing optimization; Mixed-Integer Non-linear Programming; MINLP; Modified OA/ER algorithm; multi-level MINLP strategies; steel structures; trusses

Citation: Šilih, S.; Kravanja, Z.; Kravanja, S. The MINLP Approach to Topology, Shape and Discrete Sizing Optimization of Trusses. *Appl. Sci.* **2022**, *12*, 1459. https://doi.org/10.3390/app12031459

Academic Editor: Nikos D. Lagaros

Received: 20 December 2021
Accepted: 26 January 2022
Published: 29 January 2022

1. Introduction

Optimization of different processes and systems has become an important factor in every aspect of human life, especially in the fields of science, industry and business. Numerous attempts have been made in the past in order to improve the efficiency and economic viability of structures in structural engineering. Although the beginnings of modern structural optimization go back to the end of the 19th century [1,2], the more intensive growth of the topic started in the early 1960s [3], closely linked with the progress of computer capabilities. The first attempts in the field of structural optimization were applied to solve the continuous sizing and shape optimization of structures, where all variables were treated as continuous ones. However, at the end of the previous millennium, many efficient optimization techniques were developed for solving the discrete/continuous topology, shape and discrete dimension optimization. These techniques were developed particularly for the solution of real engineering structures with discrete/standard dimensions. Although the explicit inclusion of discrete variables in the models considerably increases the extensiveness and the combinatoric complexity of the optimization problems, such a discrete/continuous type of the optimization usually proves to be very efficient with respect to both the obtained results and the required computational time.

The present paper discusses the simultaneous topology, shape and discrete/standard dimension optimization of trusses using the Mixed-Integer Non-linear Programming

(MINLP) approach. The general MINLP model formulation for truss structures is presented. This discrete/continuous non-convex and non-linear optimization problem is proposed to be solved by the Modified Outer-Approximation/Equality-Relaxation (OA/ER) algorithm by Kravanja and Grossmann [4]. In addition, some multi-level MINLP strategies that significantly accelerate the convergence of the optimization are presented. The suitability and efficiency of the proposed method are shown through some numerical examples.

2. Optimization of Trusses

Trusses are probably the most frequent grid-like structures to be applied for testing different optimization techniques since the early 1960s [3]. Compared to other types of structures, the analysis and design processes of trusses are relatively simple and can be easily written into a mathematical model. On the other hand, trusses are usually composed from a large number of elements (bars) and are, therefore, unsuitable for optimization by repeating the calculation of all different structural alternatives. In the case of real engineering trusses, a lot of bars are oversized and thus not fully exploited. These structures consequently offer numerous possibilities for improvement and optimization.

In general, truss optimization problems can be divided into two main spheres of activity. The first one belongs to the topology optimization where an optimal structure with an optional number and configuration of structural elements inside a defined superstructure has to be defined, while the second one presents a discrete sizing optimization problem, where the cross-sections of elements are forced to have discrete, in most cases standard, dimensions. Both mentioned optimization spheres represent the greatest challenge to the problem of truss optimization. In the last decades, some effective attempts of the topology and discrete dimension optimization of trusses have been made. A brief review and a history of different optimization techniques for solving these optimization problems are discussed in the following sub-sections.

2.1. Topology Optimization

The first examples of truss optimization included only sizing optimization, i.e., the calculation of optimal cross-section areas of bars. Soon after that, it was discovered that it would be reasonable to exclude some unfavorable or needless elements from the original truss structure. As a result, not only the optimal cross-sections would be obtained but also the optimal number and configuration of bars, namely the optimal topology. One of the most important contributions to the area of truss topology optimization is the so-called ground structure approach [5], where a grid of nodes and a set of inter-connections between nodes, representing bars, are defined. In the process of optimization, some bars are eliminated, and the optimal topology is represented by the sub-set of existing bars. Since trusses are analyzed using joint equilibrium equations, the set of feasible solutions includes only statically determinate structures. Further, only stress constraints are applied, and consequently, the problem can be formulated as a linear programming (LP) problem.

By including the deflection constraints and statically indeterminate solutions, the discussed truss problem becomes a non-linear one. Numerous topology optimization problems of trusses, solved by the non-linear programming (NLP) approach, were therefore subsequently presented [6–11]. Using continuous optimization methods, i.e., the LP or the NLP, the truss topology optimizations were performed by either allowing zero values or by defining a small lower bound of the cross-section areas of bars. While the former approach caused problems to be potentially insoluble due to the possible appearance of singularities, the latter generally lead to non-exact solutions, which require reanalysis. Moreover, allowing zero or non-zero values led to non-convexities, which usually cause the optimization to become stuck in poor local optima.

All the mentioned difficulties led to the idea to optimize the truss topology by different discrete optimization methods. The topology is optimized inside a discrete space by introducing binary 0–1 variables. An extra binary variable y is associated with each truss element, indicating whether this particular element is included in (y = 1) or excluded

from ($y = 0$) the current topology. By means of discrete optimization, numerous authors optimize the truss topology applying the genetic algorithm (GA) [12–16], the penalty function method [10] and the simulated annealing [17–19].

The nature of the considered truss topology problem is that the optimization models are mixed discrete/continuous, with discrete variables for topology and continuous variables for cross-section dimensions, nodal coordinates, stresses, strains, etc. As the NLP is regarded as the most effective for solving continuous non-linear optimization problems, some attempts have been made to link the NLP with different discrete optimization techniques. Such examples are the linkage of GA and NLP [20] and the tabu search [21].

Besides the widely used ground structure approach, a second approach to topology optimization of trusses is the homogenization method [22–25], where the optimal material distribution in a continuous design domain is determined and interpreted as a discrete truss.

2.2. Discrete Sizing Optimization

The first ideas for the sizing optimization of trusses by considering available discrete dimensions were presented in the late 1960s [26]. However, as the main focus in the 1960s and 1970s was on the development of efficient algorithms for solving large-scale NLP problems, the intense progress in discrete optimization methods did not start until the 1980s. The first attempts of the discrete sizing optimization of trusses were based on linear programming, e.g., Templeman's algorithm [27,28], followed by the solving of NLP problems with sequential linear programming (sequential linearization algorithm) [29–31].

In addition, practically all the developed discrete optimization techniques were applied to the truss problems, e.g., the genetic algorithm [32–34], simulated annealing [35,36], the penalty function method [37,38] and neuron networks [39]. In some cases, multi-level approaches were presented where the continuous optimization was performed at the first level, and the obtained continuous solution was used as a starting point for the subsequent discrete optimization, e.g., [30–32,40,41].

In most of the mentioned references, trusses were optimized by considering stress and deflection constraints and either without or by considering the simplified Euler buckling constraints. Cross-section areas were regarded as independent sizing variables, and a set of discrete values of the section areas (in some cases, based on the available sections) was defined. Taking this into account, researchers thus focused mainly on testing different optimization techniques, while the practical applicability of the obtained results was often kept in the background. One of the exceptions was presented in [42], where the trusses were optimized by considering the design constraints in accordance with Eurocode 3 [43] and by considering standard steel tubes as the cross-sections of elements.

2.3. Simultaneous Topology and Discrete Dimension Optimization

The first attempts to simultaneously optimize both the truss topology and the discrete dimensions of members have been presented at the beginning of this century. The problem was either simplified/linearized and was solved using the Mixed-Integer Linear Programming (MILP) and the Mixed-Logic Linear Programming (MLLP) [44] or in the non-linear form using the relative quotient algorithm [45]. In both cases [44,45], the topology was optimized by using the previously discussed method of allowing a small lower bound on the cross-section areas. In the next attempt, the truss problem was solved by employing a mixed variable formulation (MILP), where truss member buckling constraints became linear [46].

The simultaneous topology and discrete cross-section optimization of trusses was also solved by using the NLP with heuristics [47], the relative difference quotient algorithm [48], the genetic algorithm [49,50], the ant colony approach [51,52], the improved genetic algorithm with two-level approximation [53], the mixed-integer second-order cone programming approach [54], the integrated particle swarm optimizer [55], the modified meta-heuristics with random mutation [56], the advanced Jaya algorithm [57], and by the mixed integer linear optimization (MILO) [58].

2.4. MINLP Approach to Truss Synthesis

Considering the optimization of trusses, the Mixed-Integer Non-linear Programming (MINLP) approach was, in the past, applied to discrete dimension optimization only [29–31] and was seldom used for the topology optimization. The simultaneous topology and discrete sizing optimization represents an extensive non-convex and non-linear discrete/continuous optimization problem that cannot be solved without suitable MINLP algorithms and strategies. The practical applicability of the MINLP approach to structural optimization was, for example, presented in [59,60] and employed for the simultaneous topology and standard dimension optimization of hydraulic steel gates [61,62], single-story steel building structures [63] and composite floor structures [64].

The present paper introduces the structural synthesis of trusses performed by the MINLP optimization approach. Truss synthesis is performed through three steps; see also [59]. The first is the generation of a truss superstructure for different structure/topology and other design alternatives that are all candidates for a feasible and optimal solution. The second is the development of a special MINLP model formulation for the defined truss superstructure in an equation-oriented environment. The last step is the solution of the defined MINLP model, performed by a suitable MINLP algorithm and strategies, which, in the simultaneous MINLP optimization approach, yields an optimal solution.

As a result of the simultaneous optimization procedure, the MINLP truss synthesis yields:

- the optimal structure mass or costs as the defined objective;
- the optimal truss topology with the optimal number and configuration of bars;
- the optimal joint coordinates, which define the shape of the truss; and
- the optimal discrete/standard cross-section dimensions of bars.

While the structure mass and joint coordinates represent continuous parameters, which are optimized inside the continuous space, the optimization of topology and discrete/standard dimensions require discrete decisions. The discussed truss synthesis thus corresponds to a mixed discrete/continuous non-linear optimization problem, which can be solved by the MINLP.

3. Development of the MINLP Model Formulation for Truss Superstructures

Truss synthesis requires the generation of an MINLP truss superstructure, which includes all possible topology/structure alternatives to compete for a feasible and optimal solution. The truss superstructure consists of the provided set of nodes and their interconnections, which represent the elements of the truss, i.e., bars. Special logical relations between the elements have been defined in order to provide the kinematical stability of the structure and prevent the undesirable overlapping of elements involved in different topology/structure alternatives. In general, all nodes and elements are alternative (optional), i.e., they can be selected or rejected from the structure. Some nodes, however, e.g., supported nodes and those where nodal loads are applied, are fixed and included in all alternative truss designs. The fixed nodes together with some fixed elements reduce the combinatorial expanse of the optimization problem. Besides topological alternatives, the discrete/standard dimension alternatives are also defined in the superstructure. Although a high number of discrete/standard alternatives, in general, leads to better results, it also leads to extensive models and very expensive and difficult-to-solve problems.

3.1. The General MINLP Problem Formulation

The MINLP truss superstructure is modeled as an MINLP problem in which continuous and discrete variables are handled simultaneously. Continuous variables are defined for the continuous optimization of parameters, while discrete variables are used for discrete/standard dimensions and to express discrete decisions, i.e., the existence or non-

existence of alternative structural elements. The general non-linear continuous/discrete optimization problem (MINLP-G) can be formulated as follows:

$$\min z = \boldsymbol{c}^{\mathrm{T}}\boldsymbol{y} + f(\boldsymbol{x})$$

$$\text{s.t.}$$

$$\boldsymbol{h}(\boldsymbol{x}) = \boldsymbol{0}$$

$$\boldsymbol{g}(\boldsymbol{x}) \leq \boldsymbol{0} \qquad \text{(MINLP-G)}$$

$$\boldsymbol{B}\boldsymbol{y} + \boldsymbol{C}\boldsymbol{x} \leq \boldsymbol{b}$$

$$\boldsymbol{x} \in X = \{\boldsymbol{x} \in R^n \colon \boldsymbol{x}^{\mathrm{LO}} \leq \boldsymbol{x} \leq \boldsymbol{x}^{\mathrm{UP}}\}$$

$$\boldsymbol{y} \in Y = \{0,1\}^m$$

where $\boldsymbol{x}$ is a vector of continuous variables specified in the compact set X and $\boldsymbol{y}$ is a vector of binary 0–1 variables. Functions $f(\boldsymbol{x})$, $\boldsymbol{h}(\boldsymbol{x})$ and $\boldsymbol{g}(\boldsymbol{x})$ are continuous and differentiable non-linear functions involved in the objective function, equality and inequality constraints, respectively. Finally, $\boldsymbol{B}\boldsymbol{y} + \boldsymbol{C}\boldsymbol{x} \leq \boldsymbol{b}$ represents a sub-set of mixed linear equality/inequality constraints.

It should be noted that in the context of truss synthesis, continuous variables define continuous structure parameters such as nodal coordinates, internal forces, deflections, etc., while binary variables represent the potential existence of structural elements and discrete dimensions inside the truss superstructure. Equality and inequality constraints represent a rigorous system of functions taken from structural analysis. Logical constraints that must be fulfilled for discrete decisions and structure configurations are given by $\boldsymbol{B}\boldsymbol{y} + \boldsymbol{C}\boldsymbol{x} \leq \boldsymbol{b}$. The objective function to be minimized represents the purpose of the optimization (e.g., mass or cost minimization) and is generally composed from a linear part $\boldsymbol{c}^{\mathrm{T}}\boldsymbol{y}$, which depends on the number of selected structural elements (those with non-zero binary variables), and from the non-linear dimension dependent part $f(\boldsymbol{x})$.

3.2. The MINLP Model Formulation for Truss Superstructures

The above-mentioned general formulation MINLP-G was adopted for truss synthesis. As a result, the MINLP truss superstructure formulation MINLP-TS was developed. As a basis for the MINLP-TS formulation, the already developed continuous NLP truss optimization model was used. The NLP model proved successful for the continuous shape and sizing optimization of steel trusses [65], composite trusses [66] and timber trusses by considering joint flexibility [67].

The proposed MINLP-TS model formulation for planar truss superstructures consists of the objective function, structural analysis and logical constraints with continuous and binary variables:

Objective function:

$$\min MASS = \rho \cdot \sum_{i=1}^{n} \sum_{\substack{j=1 \\ el_{i,j}=1}}^{n} A_{i,j}^{\mathrm{sf}} \cdot s_{i,j}^{\mathrm{sf}} \tag{1}$$

subjected to:

Structural analysis constraints:

Boundary constraints:

$$u_{k,i} = 0,\ k \in K,\ \forall\, i \in I \big| \mathrm{s_{x},}_i = 1 \tag{2}$$

$$v_{k,i} = 0,\ k \in K,\ \forall\, i \in I \big| \mathrm{s_{y},}_i = 1 \tag{3}$$

$$F_{x,k,i} = p_{x,k,i},\ k \in K,\ \forall\, i \in I \Big| s_{x,i} = 0 \tag{4}$$

$$F_{y,k,i} = p_{y,k,i},\ k \in K,\ \forall\, i \in I \Big| s_{y,i} = 0 \tag{5}$$

Finite element equations:

$$\begin{matrix} \sum\limits_{\substack{j=1 \\ el_{i,j}=1}}^{n} \frac{A_{i,j}^{sf} \cdot E}{s_{i,j}^{sf}} \cdot \left[l_{i,j}^{sf\,2} \cdot \left(u_{k,i} - u_{k,j} \right) + l_{i,j}^{sf} \cdot m_{i,j}^{sf} \cdot \left(v_{k,i} - v_{k,j} \right) \right] + \\ \sum\limits_{\substack{j=1 \\ el_{j,i}=1}}^{n} \frac{A_{j,i}^{sf} \cdot E}{s_{j,i}^{sf}} \cdot \left[l_{j,i}^{sf\,2} \cdot \left(u_{k,i} - u_{k,j} \right) + l_{j,i}^{sf} \cdot m_{j,i}^{sf} \cdot \left(v_{k,i} - v_{k,j} \right) \right] = F_{x,k,i} \end{matrix} \quad k \in K,\ i \in I \tag{6}$$

$$\begin{matrix} \sum\limits_{\substack{j=1 \\ el_{i,j}=1}}^{n} \frac{A_{i,j}^{sf} \cdot E}{s_{i,j}^{sf}} \cdot \left[l_{i,j}^{sf} \cdot m_{i,j}^{sf} \cdot \left(u_{k,i} - u_{k,j} \right) + m_{i,j}^{sf\,2} \cdot \left(v_{k,i} - v_{k,j} \right) \right] + \\ \sum\limits_{\substack{j=1 \\ el_{j,i}=1}}^{n} \frac{A_{j,i}^{sf} \cdot E}{s_{j,i}^{sf}} \cdot \left[l_{j,i}^{sf} \cdot m_{j,i}^{sf} \cdot \left(u_{k,i} - u_{k,j} \right) + m_{j,i}^{sf\,2} \cdot \left(v_{k,i} - v_{k,j} \right) \right] = F_{y,k,i} \end{matrix} \quad k \in K,\ i \in I \tag{7}$$

$$\frac{A_{i,j}^{sf} \cdot E}{s_{i,j}^{sf}} \cdot \left[l_{i,j}^{sf} \cdot \left(u_{k,i} - u_{k,j} \right) + m_{i,j}^{sf} \cdot \left(v_{k,i} - v_{k,j} \right) \right] = -F_{k,i,j},\ k \in K,\ \forall\, (i,j) | el_{i,j} = 1 \tag{8}$$

Substituted functions:

$$A_{i,j}^{sf} = f\left(d_{i,j}\right),\ \forall\, (i,j) \Big| el_{i,j} = 1 \tag{9}$$

$$s_{i,j}^{sf} = \sqrt{\left({}^{c}x_j - {}^{c}x_i\right)^2 + \left({}^{c}y_j - {}^{c}y_i\right)^2},\ \forall\, (i,j) \Big| el_{i,j} = 1 \tag{10}$$

$$l_{i,j}^{sf} = \left({}^{c}x_j - {}^{c}x_i\right) / s_{i,j}^{sf},\ \forall\, (i,j) \Big| el_{i,j} = 1 \tag{11}$$

$$m_{i,j}^{sf} = \left({}^{c}y_j - {}^{c}y_i\right) / s_{i,j}^{sf},\ \forall\, (i,j) \Big| el_{i,j} = 1 \tag{12}$$

Design constraints

$$F_{k,i,j} \le A_{i,j}^{sf} \cdot \sigma^{t,max},\ k \in K\ \forall\, (i,j) \Big| el_{i,j} = 1 \tag{13}$$

$$F_{k,i,j} \ge -A_{i,j}^{sf} \cdot \sigma^{c,max},\ k \in K\ \forall\, (i,j) \Big| el_{i,j} = 1 \tag{14}$$

$$F_{k,i,j} \ge -A_{i,j}^{sf} \cdot \sigma_{i,j}^{cr},\ k \in K\ \forall\, (i,j) \Big| el_{i,j} = 1 \tag{15}$$

Deflection constraints

$$u_{k,i} \le u_i^{max},\ k \in K\ i \in I \tag{16}$$

$$v_{k,i} \le v_i^{max},\ k \in K\ i \in I \tag{17}$$

Logical constraints:
Inter-connection logical constraints:

$$\boldsymbol{B}\boldsymbol{y}^{top} \le \boldsymbol{b} \tag{18}$$

Bound logical constraints:

$$d_{i,j} - d_{i,j}^{UP} \cdot y_{i,j}^{top} \le 0,\ \forall\, (i,j) \Big| el_{i,j} = 1 \tag{19}$$

$$d_{i,j} - \mathrm{d}_{i,j}^{\mathrm{ex,LO}} \cdot y_{i,j}^{\mathrm{top}} \geq 0,\ \forall\ (i,j) \Big| el_{i,j} = 1 \tag{20}$$

Logical relations for common variables:

$$d_{i,j} \geq d_g^{\mathrm{com}} - \mathrm{d}_{i,j}^{\mathrm{UP}} \cdot \left(1 - y_{i,j}^{\mathrm{top}}\right),\ \forall\ (g,i,j) \Big| gel_{g,i,j} = 1 \tag{21}$$

$$d_{i,j} \leq d_g^{\mathrm{com}} + \mathrm{d}_{i,j}^{\mathrm{UP}} \cdot \left(1 - y_{i,j}^{\mathrm{top}}\right),\ \forall\ (g,i,j) \Big| gel_{g,i,j} = 1 \tag{22}$$

Logical relations for discrete dimensions:

$$d_{i,j} = \sum_{l \in L} q_{i,j,l} \cdot y_{i,j,l}^{\mathrm{st}},\ \forall\ (i,j) | el_{i,j} = 1 \tag{23}$$

$$\sum_{l \in L} y_{i,j,l}^{\mathrm{st}} = y_{i,j}^{\mathrm{top}},\ \forall\ (i,j) | el_{i,j} = 1 \tag{24}$$

Variables:

$$(\mathrm{d}_{i,j}^{\mathrm{LO}} = 0) \leq d_{i,j} \leq \mathrm{d}_{i,j}^{\mathrm{UP}},\ \forall\ (i,j) \Big| el_{i,j} = 1$$

$${}^{\mathrm{c}}\mathrm{x}_i^{\mathrm{LO}} \leq {}^{\mathrm{c}}x_i \leq {}^{\mathrm{c}}\mathrm{x}_i^{\mathrm{UP}},\ i \in I$$

$${}^{\mathrm{c}}\mathrm{y}_i^{\mathrm{LO}} \leq {}^{\mathrm{c}}y_i \leq {}^{\mathrm{c}}\mathrm{y}_i^{\mathrm{UP}},\ i \in I$$

$$y_{i,j}^{\mathrm{top}} \in \{0,1\},\ \forall\ (i,j) \Big| el_{i,j} = 1$$

$$y_{i,j,l}^{\mathrm{st}} \in \{0,1\},\ l\ \in L,\ \forall\ (i,j) \Big| el_{i,j} = 1$$

A detailed description of the MINLP-TS model formulation is given in the following sub-sections.

3.2.1. Definition of Structural Elements

The basis of the truss superstructure is composed by n defined nodes, $n \in N$. Each alternative truss element is defined as an inter-connection between two nodes: for each pair of nodes i and j, where $i \in I = \{1,2,3, \ldots\ n\}$ and $j \in J = \{1,2,3, \ldots\ n\}$ and $i < j$, an element coefficient $el_{i,j}$ is defined. The coefficient $el_{i,j}$ is valued 1, if an alternative element (bar) exists connecting nodes i and j (in the following text denoted as $i \rightarrow j$); otherwise, $el_{i,j}$ is equal to zero. An $n \times n$ truss element matrix **EL** is then formed from coefficients $el_{i,j}$. The definition of a truss element and its position in the global coordinate system XY is shown in Figure 1.

3.2.2. Variables

The MINLP-TS model formulation includes continuous variables as well as discrete binary variables. In general, continuous variables are partitioned into independent (design) variables and into dependent (non-design) variables. In the specific case of truss synthesis, the design variables are sizing variables (i.e., dimensions of the cross-sections of bars, $d_{i,j}$) and shape variables (i.e., nodal coordinates ${}^{\mathrm{c}}x_i$ and ${}^{\mathrm{c}}y_i$). These variables define the structural design. Non-design performance variables are directly dependent on the design variables and represent the cross-section properties, internal forces, deformations, resistances of bars, etc.

Discrete variables are represented by a vector of binary variables $\boldsymbol{y} = \{\boldsymbol{y}^{\mathrm{top}}, \boldsymbol{y}^{\mathrm{st}}\}$, where sub-vectors $\boldsymbol{y}^{\mathrm{top}}$ and $\boldsymbol{y}^{\mathrm{st}}$ stand for the topological and discrete/standard dimension binary variables, respectively. In the first sub-vector, topological binary variables $y_{i,j}^{\mathrm{top}}$ are defined for all alternative structural elements involved in the superstructure. Topological binary variables are subsequently partitioned into those defining nodes ($y_{i,j}^{\mathrm{top}}$, $I = j$, further on in the text $y_{i,i}^{\mathrm{top}}$) and into those defining bars ($y_{i,j}^{\mathrm{top}}$, $\forall\ (i,j)\ |\ el_{i,j} = 1$). Each topological binary variable represents the existence or selection ($y_{i,j}^{\mathrm{top}} = 1$) or non-existence or rejection ($y_{i,j}^{\mathrm{top}} = 0$) of its associated structural element.

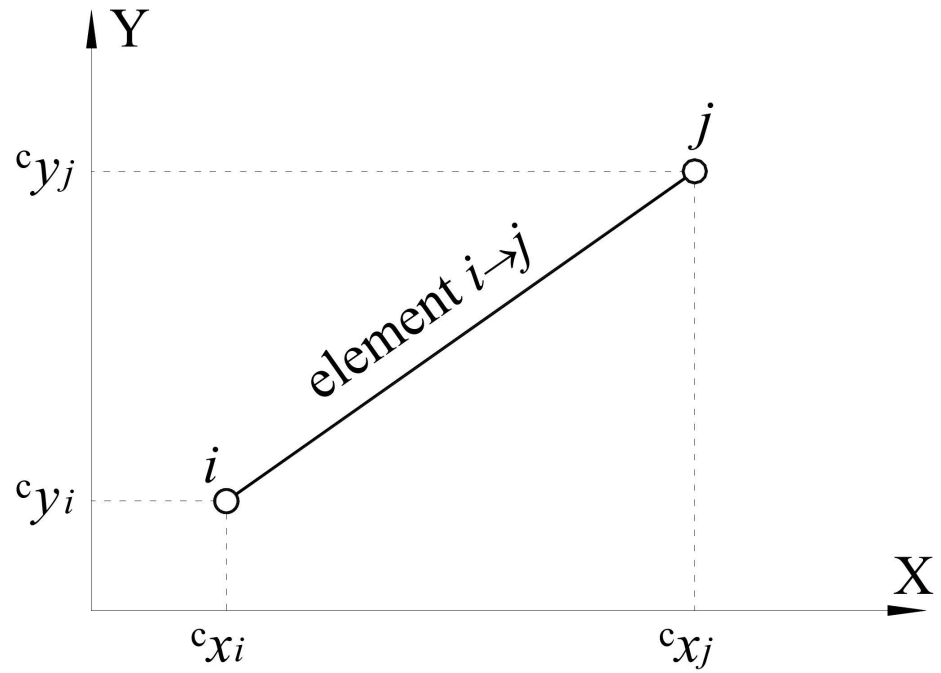

Figure 1. Definition of a truss element.

The second sub-vector of binary variables contains binary variables attributed to the discrete/standard dimensions. Let L be a set of discrete/standard alternatives of a particular cross-section dimension. A binary variable $y^{\mathrm{st}}_{i,j,l}$ is then defined for each discrete cross-section alternative l, $l \in L$, for each bar element $i \rightarrow j$.

3.2.3. Objective Function

In the present truss synthesis, the objective function Equation (1) represents the mass of the truss superstructure, where ρ denotes the unit mass of the material and $A^{\mathrm{sf}}_{i,j}$ and $s^{\mathrm{sf}}_{i,j}$ are the cross-section area and the length of element $i \rightarrow j$, respectively.

In its simplest form, the objective function can be linear, when the cross-section areas of bars are considered as independent sizing variables and the joint coordinates of the truss are fixed (i.e., the lengths of the elements are fixed parameters). In the engineering structures, however, the bars are built from standard cross-sections. Each cross-section area generally depends on several dimensions. This is important, especially when buckling constraints are included, as buckling resistance of a bar is dependent not only on its cross-section area but also on the shape and individual dimensions of its cross-section. By considering circular hollow sections (tubes), for example, each cross-section is defined by two independent sizing variables, i.e., the tube diameter $d_{i,j}$ and the wall thickness $t_{i,j}$. The cross-section area is therefore evaluated from the cross-section dimensions and in the constraints defined as a substituted function $A^{\mathrm{sf}}_{i,j}$; see Equation (9). In addition, when the shape of the structure is also optimized, the joint coordinates become variables, and consequently, the lengths of the bars also become substituted functions $s^{\mathrm{sf}}_{i,j}$; see Equation (10). In effect, the mass of the structure becomes a non-linear function (Equation (1a)):

$$MASS = \rho \cdot \pi \cdot \sum_{i=1}^{n} \sum_{\substack{j=1 \\ el_{i,j}=1}}^{n} \left[t_{i,j} \cdot \left(d_{i,j} - t_{i,j} \right) \cdot \sqrt{\left({}^{\mathrm{c}}x_j - {}^{\mathrm{c}}x_i \right)^2 + \left({}^{\mathrm{c}}y_j - {}^{\mathrm{c}}y_i \right)^2} \right] \tag{1a}$$

where $d_{i,j}$ and $t_{i,j}$ denote the tube diameter and the wall thickness of element $i \rightarrow j$, respectively, and ${}^{\mathrm{c}}x_i$, ${}^{\mathrm{c}}x_j$, ${}^{\mathrm{c}}y_i$ and ${}^{\mathrm{c}}y_j$ are the coordinates of joints i and j.

3.2.4. Structural Analysis Constraints

Non-linear and linear parameter constraints (Equations (2)–(17)) as well as the lower and upper bounds on continuous variables represent a rigorous system of functions taken from structural analysis. In the proposed MINLP formulation, structural analysis constraints are divided into boundary constraints, finite element equations, design constraints and deflection constraints.

The boundary constraints, Equations (2)–(5), define the supporting and loading conditions of the structure. The supporting conditions are established through coefficients $s_{x,i}$ and $s_{y,i}$ defined for each node i. The coefficient $s_{x,i}$ is valued 1 if node i is supported in the direction of axis X; otherwise, it is valued 0. Similarly, $s_{y,i}$ is 1 when node i is supported in Y direction. Consequently, the corresponding deflections of the supported nodes are defined to be zero by Equations (2) and (3). The load on a truss is given by the nodal forces, which are defined by the loading coefficients $p_{x,k,i}$ and $p_{y,k,i}$ in Equations (4) and (5). Each parameter $p_{x,k,i}$ contains the value of the nodal force, which acts on node i in the direction of axis X and corresponds to the loading case k, $k \in K$. In the same way, the nodal forces in the direction of axis Y are defined by coefficients $p_{y,k,i}$. In the proposed MINLP-TS formulation, the supporting and loading coefficients are arranged into a set of corresponding vectors $\boldsymbol{s}_x = \{s_{x,i}\}$, $\boldsymbol{s}_y = \{s_{y,i}\}$, $\boldsymbol{p}_{x,k} = \{p_{x,k,i}\}$ and $\boldsymbol{p}_{y,k} = \{p_{y,k,i}\}$.

The finite element equations, Equations (6)–(8), are used to calculate the reactions, axial forces and displacements of the structure. Equations (6) and (7) are defined for each node i. As node i can, in general, be either the starting or the ending joint of a bar, the contributions of elements $i \rightarrow j$ ($i < j$; i is the starting joint) as well as $j \rightarrow i$ ($j > i$; i is the ending joint) have to be considered. Parameters $l_{i,j}^{sf}$ and $m_{i,j}^{sf}$ are the cosines of the angles between the local longitudinal axis of bar $i \rightarrow j$ and the global axes X and Y, respectively. When the shape of the structure is also optimized, parameters $l_{i,j}^{sf}$ and $m_{i,j}^{sf}$ become substituted functions of the joint coordinates; see Equations (11) and (12).

The design constraints, Equations (13)–(15), represent the calculation of the stresses and buckling of bars, where $\sigma^{t,max}$ and $\sigma^{c,max}$ are the tensile and compressive strength of the material, while $\sigma_{i,j}^{cr}$ is the limit buckling stress of bar $i \rightarrow j$. It should be noted that, according to Equation (8), the positive sign of the axial force $F_{k,i,j}$ represents a tensile force. The deflection constraints, Equations (16) and (17), ensure that the deformations of joints remain within the allowed limits.

3.2.5. Logical Constraints

The purpose of the logical constraints (Equations (18)–(24)) is defining different discrete decisions related to reducing the set of topology alternatives, defining the interconnections between structural elements, establishing the bounds on continuous variables for alternative elements and linking the continuous sizing variables with discrete/standard values. It should be noted that all the logical constraints are expressed by the use of binary variables.

1. Inter-connection logical constraints. Integer equality/inequality constraints, see Equation, (18), are proposed to provide the kinematical stability of the structure, to prevent the overlapping of elements, etc. They are provided by the defining of simple relations between the corresponding topological binary variables. The inter-connection constraints can be divided into bar–bar constraints and joint–bar constraints. Some general examples of bar–bar constraints are:
   - bar $i \rightarrow j$ can be selected only if bar $i' \rightarrow j'$ is also selected: $y_{i,j}^{top} - y_{i',j'}^{top} \leq 0$;
   - if bar $i \rightarrow j$ is selected, bar $i' \rightarrow j'$ must also be selected: $y_{i,j}^{top} - y_{i',j'}^{top} = 0$;
   - bars $i \rightarrow j$ and $i' \rightarrow j'$ exclude each other, i.e., only one can be selected at the most: $y_{i,j}^{top} + y_{i',j'}^{top} \leq 1$, etc.

   An example of a joint–bar constraint is:

- bar $i \rightarrow j$ can be selected only if both of its end joints (i and j) are selected: $2 \cdot y_{i,j}^{\text{top}} \leq y_{i,i}^{\text{top}} + y_{j,j}^{\text{top}}$.

2. Bound logical constraints. Equations (19) and (20) are proposed to define the bounds of individual sizing variables $d_{i,j}$ and enforce these variables to zero values if their associated bar does not exist (the associated topological binary variable $y_{i,j}^{\text{top}} = 0$). Otherwise, the variables are subjected to the lower bounds $\mathrm{d}_{i,j}^{\text{ex,LO}}$ and to the upper bounds $\mathrm{d}_{i,j}^{\text{UP}}$ when the alternative bar exists ($y_{i,j}^{\text{top}} = 1$). It should be noted that the values of $\mathrm{d}_{i,j}^{\text{ex,LO}}$ are strictly larger than zero and should be distinguished from the actual lower bounds $\mathrm{d}_{i,j}^{\text{LO}}$, which must be zero in the case when the associated bars disappear. In this way, the cross-sectional areas of inactive bars are zero, and such bars do not contribute to the stiffness matrix of the structure and the objective function.
3. Logical relations for common variables. Although a truss is usually fully exploited when each bar has a different cross-section, it is nevertheless (e.g., for construction reasons) advantageous for some groups of bars to have equal cross-sections. Equations (21) and (22) assure that a cross-section dimension $d_{i,j}$ of each bar $i \rightarrow j$, which belongs to group g, $g \in G$, takes the value d_g^{com} when the bar is selected ($y_{i,j}^{\text{top}} = 1$). Otherwise, when $y_{i,j}^{\text{top}} = 0$, the design variables take zero values due to Equations (19) and (20), while Equations (21) and (22) become redundant. The linkage of bars to certain groups is defined through the coefficients $gel_{g,i,j}$, which take the value 1 if bar $i \rightarrow j$ belongs to group g; otherwise, they are set to value 0.
4. Logical relations for discrete/standard dimensions. The linear equality constraints, Equations (23) and (24), assure that when an element exists, the cross-section dimension $d_{i,j}$ takes one of the defined alternative discrete/standard dimension values. For each bar $i \rightarrow j$, a set of l, $l \in L$, alternative discrete dimension values $q_{i,j,1}$ are defined, and to each $q_{i,j,1}$, an extra binary variable $y_{i,j,l}^{\text{st}}$ is assigned. The dimension $d_{i,j}$ is then defined as a scalar product between a vector of the alternative discrete dimension values $\boldsymbol{q}_{i,j,l} = \{q_{i,j,1}, q_{i,j,2}, \ldots\ q_{i,j,l}\}$ and the associated vector of binary variables $\boldsymbol{y}_{i,j,l}^{\text{st}} = \left\{y_{i,j,1}^{\text{st}}, y_{i,j,2}^{\text{st}}, \ldots, y_{i,j,l}^{\text{st}}\right\}$; see Equation (23). Additionally, by Equation (24), only one discrete value can be associated to a selected bar ($y_{i,j}^{\text{top}} = 1$) and none to a rejected bar ($y_{i,j}^{\text{top}} = 0$).

4. Solution of the MINLP Truss Synthesis Problem

After the MINLP model formulation has been developed, the defined MINLP synthesis problem is solved by the use of a suitable MINLP algorithm. A general MINLP class of optimization problems (MINLP-G) can, in principle, be solved by the following algorithms and their extensions:

- Non-linear Branch and Bound method, NBB [68,69];
- LP/NLP-based Branch and Bound algorithm [70];
- Sequential Linear Discrete Programming, SLDP [30];
- Extended Cutting Plane method, ECP [71];
- Generalized Benders Decomposition [72,73];
- Outer-Approximation algorithm, OA [74];
- Feasibility Technique [75];
- Outer-Approximation/Equality-Relaxation algorithm, OA/ER, [76].

From a variety of different techniques and their individual characteristics, the OA/ER algorithm has proved to be very successful in solving large-scale MINLP problems in cases when NLP sub-problems are expensive and difficult to solve. As the MINLP problems of truss synthesis are highly non-linear, the OA/ER algorithm was selected to fulfil this task.

4.1. The Modified OA/ER Algorithm

The OA/ER algorithm comprises the solving of an alternative sequence of Non-linear Programming (NLP) optimization sub-problems and Mixed-Integer Linear Programming (MILP) master problems; see Figure 2. The former corresponds to the continuous optimization of parameters for a superstructure with fixed discrete/binary variables and yields an upper bound to the objective to be minimized. The latter involves a global approximation to the superstructure of alternatives in which new values of discrete/binary variables (new topology and standard dimensions) are identified so that its lower bound does not exceed the current best upper bound. A global linear approximation includes the linear constraints from the original MINLP problem as well as the linearizations of the non-linear objective function and the non-linear (in)equality constraints, accumulated at each NLP sub-problem solution.

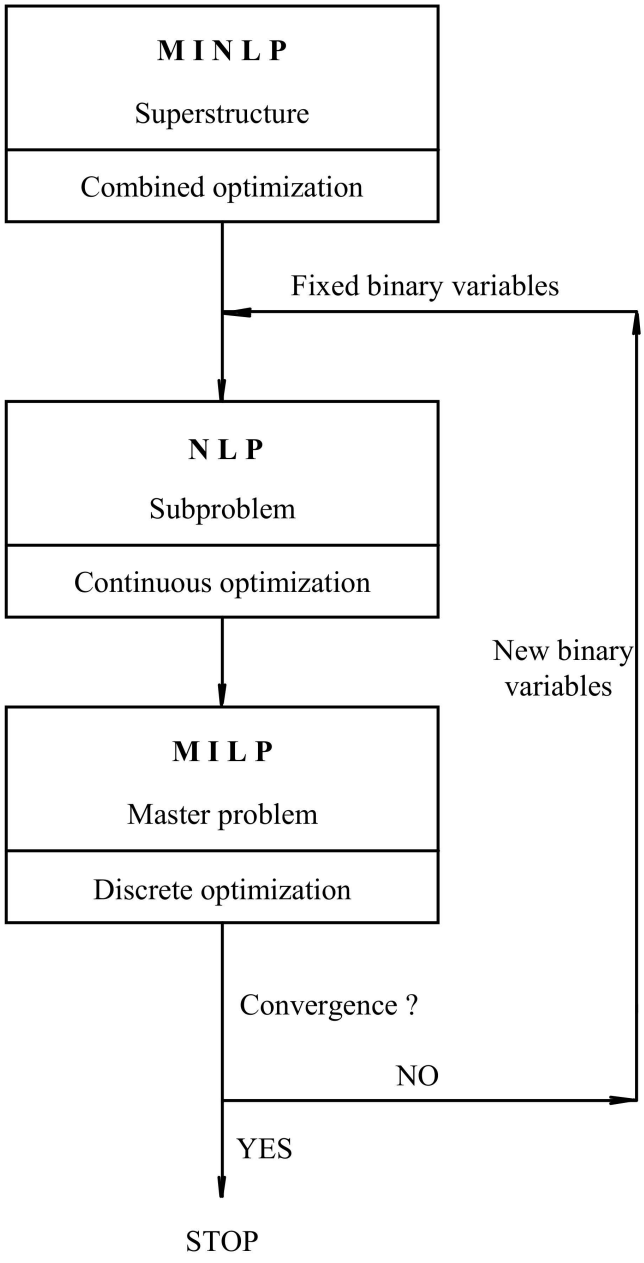

Figure 2. Steps of the Outer-Approximation/Equality-Relaxation algorithm.

The OA/ER algorithm, like all other MINLP methods, does not generally guarantee that the obtained solution is the global optimum. This is due to the presence of non-convex functions that may cut off the global optimum. In order to reduce the undesirable effects of non-convexities, a Modified OA/ER algorithm was developed by Kravanja and Grossmann [4]. The Modified OA/ER algorithm allows the following modifications to be applied to the master problem: deactivation of the linearizations, decomposition and deactivation of the objective function linearization, use of the penalty function, use of the upper bound on the objective function to be minimized as well as a global convexity test and the validation of the outer approximations; see also [59].

4.2. Multi-Level MINLP Strategies

Besides many non-linearities and non-convexities, a very high number of discrete variables, particularly those associated with discrete dimensions, may be included in the optimization. The simultaneous topology and standard dimension optimization can generally be performed in a single MINLP phase. With the Single-Phase MINLP approach [77], the optimal result is reached directly in a single optimization process together with the optimal topology and standard dimension. All the binary variables included in the optimization are initialized in a single full set. The disadvantage of this approach is that the initialization scheme is weak, since the chosen initial standard dimensions may be infeasible or a bad choice. This strategy also exhibits slow convergence when applied to large-scale MINLP problems, and the result obtained may be a poor local solution. In order to overcome these problems, we applied multi-level MINLP [60,77–80]. From a number of multi-level strategies, two were applied to truss synthesis:

1. The Two-Phase (TP) MINLP approach [80], and
2. The Linked Two-Phase (LTP) MINLP strategy [60].

The TP approach performs topology, shape and standard dimension optimization separately in two phases. In the first phase, the simultaneous topology, shape and continuous sizing optimization is performed with the dimensions of the cross-sections being temporarily relaxed into continuous parameters. When the optimal topology is obtained, the discrete dimensions of cross-sections are re-established, and the process continues with the second phase, where the shape and standard dimension optimization is performed until the optimal solution is obtained. In the second phase, the optimization is carried out at the fixed optimal topology obtained in the first phase. The TP approach is thus performed through a hierarchic decomposition of discrete binary variables into two sub-sets. The first sub-set is used to describe topology alternatives and the second one to describe discrete dimension alternatives.

The main disadvantage of the TP strategy lies in the fact that the final solution is not necessarily the optimal one since the topology and standard dimensions are optimized consecutively. A simultaneous consideration of the standard dimensions may cause a change in the optimal topology [60]. In order to avoid the disadvantages of the TP approach, the LTP strategy was developed. While the first phase of the LTP strategy is identical to the first phase of the TP approach, the second phase differs in the fact that by using the LTP strategy, the topology is not fixed. The second phase of the LTP strategy thus performs simultaneous topology, shape and standard dimension optimization.

As the majority of binary variables is attributed to discrete/standard dimensions, the design space in the previously described second phases is still very extensive, and in some cases, even when the TP strategy is used, a very high number of MINLP iterations is needed before the first feasible solution is attained. In order to additionally reduce the discrete space, after the first phase is complete (topology optimization with continuous sizing variables), a special pre-screening of the discrete dimensions is applied. With the use of the pre-screening procedure the discrete solution is sought only in some pre-defined neighborhood of the continuous solution obtained in the first phase.

4.3. Pre-Screening of Discrete/Standard Dimensions

In order to reduce the number of binary variables attributed to discrete dimensions and considering the fact that the optimal discrete dimensions are expected to be near the optimal continuous dimensions obtained in the previous phase, the pre-screening technique was applied after the first phase (after obtaining the optimal topology and continuous sizes).

The alternative discrete dimension values in the vector $\boldsymbol{q}_{i,j,l} = \{q_{i,j,1}, q_{i,j,2}, \dots\ q_{i,j,l}\}$ from Equation (23) are positioned from the smallest discrete value in the first position to the largest value in the last position. A special parameter $l_{i,j}^{\mathrm{ps}}$ is then defined for each bar $i \rightarrow j$ at the m–th MINLP iteration (MINLP^m, $m \in M$), as a $\boldsymbol{q}_{i,j,l}$ vector's position counter l, $l \in L$, where the continuous dimension $d_{i,j}^{m-1}$, obtained in the previous NLP^{m-1} sub-problem, is positioned next to its discrete standard value $q_{i,j,l}$; see Equation (25). The subsequent initialization of binary variables $y_{i,j,l}^{st}$ for standard dimensions is for the current MILP^m master problem, then performed by Equation (26):

$$l_{i,j}^{\mathrm{ps}} = l,\ q_{i,j,l} \le d_{i,j}^{m-1} < q_{i,j,l+1},\ \forall\ (i,j) \Big| el_{i,j} = 1 \tag{25}$$

$$\begin{array}{rll} y_{i,j,l}^{\mathrm{st}} = 0 & \text{if} & l - l_{i,j}^{\mathrm{ps}} > n^{\mathrm{ps}+} \\ 0 \le y_{i,j,l}^{\mathrm{st}} \le 1 & \text{if} & n^{\mathrm{ps}-} \le l - l_{i,j}^{\mathrm{ps}} \le n^{\mathrm{ps}+} \\ y_{i,j,l}^{\mathrm{st}} = 0 & \text{if} & l - l_{i,j}^{\mathrm{ps}} < n^{\mathrm{ps}-} \end{array} \tag{26}$$

where $n^{\mathrm{ps}-}$ and $n^{\mathrm{ps}+}$, close to the previously obtained continuous dimension $d_{i,j}^{m-1}$, define the number of neighboring lower and upper discrete dimensions, which will take an active part in the subsequent discrete sizing optimization. The binary variables lying inside the neighborhood limited by $n^{\mathrm{ps}-}$ and $n^{\mathrm{ps}+}$ are hence active ($0 \le y_{i,j,l}^{\mathrm{st}} \le 1$), while the rest of them are deactivated, i.e., set to zero ($y_{i,j,l}^{\mathrm{st}} = 0$). In this way, only the reduced set of active binary variables is involved in the optimization that significantly decreases the discrete combinatorial problem.

4.4. The Proposed MINLP Strategies for Truss Synthesis

Both the TP and LTP multi-level MINLP strategies were applied to truss synthesis problems. The TP approach yielded good solutions in a few MINLP iterations. In the use of the LTP strategy, however, no feasible solutions were obtained in reasonable CPU times. The search space in the second phase proved to be too extensive. Moreover, due to the nature of truss structures, the pre-screening of standard dimensions cannot be performed effectively because only elements selected from the first phase topology can provide useful information for the subsequent second phase.

As mentioned before, by using the Two-Phase MINLP strategy, the optimal topology obtained in the first phase (topology and continuous sizing optimization) is adopted as the final optimal topology. The possible change in topology due to the inclusion of discrete sizing variables in the second phase is thus prevented. In order to allow the topology to be changed after the activation of discrete sizing variables and in order to gain information of the influence of their inclusion on the subsequent optimization, some modifications were introduced into the TP strategy. Two varieties of the TP strategy are thus proposed: the Modified Two-Phase MINLP strategy and the Sequential Two-Phase MINLP strategy. Both strategies are described in the following sub-sections.

4.4.1. The Modified Two-Phase (MTP) MINLP Strategy

The Modified TP strategy (see Figure 3) starts (at $n = 1$) with topology, shape and sizing optimization where cross-section dimensions are relaxed into continuous parameters (MINLP phase T). The process proceeds until the convergence of the OA/ER algorithm is achieved, i.e., when the lower bound, obtained at the MILP master problem, exceeds the upper bound yielded by the best NLP sub-problem. The obtained topology (with the theoretical value of the objective z_n^{t}) is adopted as the optimal topology of the first

phase. After that, the pre-screening of discrete dimensions for selected bars is applied. The calculation process proceeds with the second phase (MINLP phase D), where the shape and discrete sizing optimization is performed at the fixed optimal topology from the first phase. The obtained solution (with the discrete value of the objective z_n^{d}) now represents the structure with optimal topology, shape and discrete/standard values of cross-section dimensions ($z_{\mathrm{OPT}} = z_n^{\mathrm{d}}$). Up to this stage, the process coincides with the classical Two-Phase MINLP approach. However, by terminating the process at this point, one would not gain any information about the possible influence of the incorporation of discrete sizing variables on the subsequent topology optimization.

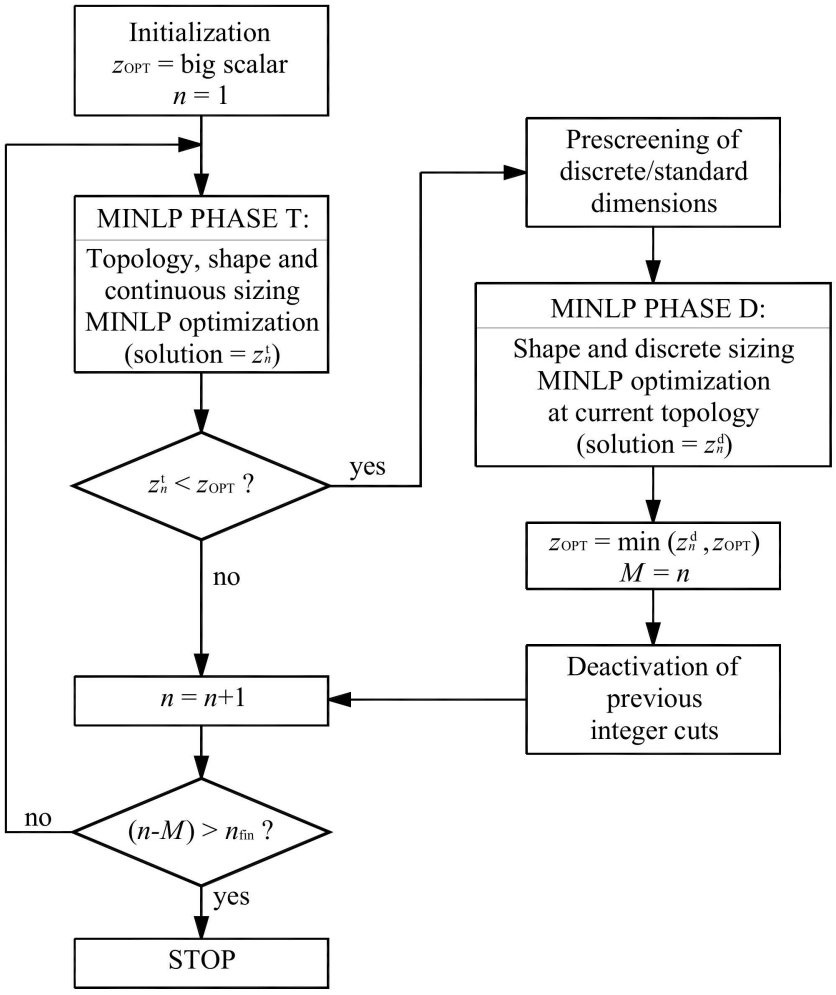

Figure 3. The Modified Two-Phase (MTP) MINLP strategy.

The process is therefore returned back to the first phase with the topology optimization in which the discrete sizing variables are again relaxed into continuous parameters. At this stage, the accumulated linearizations of the previous discrete sizing optimization phase are also included in the optimization. As the »integer cut« equations prevent all topologies obtained in previous iterations from being re-calculated, former topologies are now excluded from the superstructure, which may cut off some good solutions. For this reason, all the integer cuts with the exception of the one resulting from the optimal topology are thus deactivated after the conclusion of the initial Two-Phase procedure.

In the continuation ($n = n + 1$), each time a topology is obtained, which would yield a theoretical objective value z_n^{t} better than the current optimal solution ($z_n^{\mathrm{t}} < z_{\mathrm{OPT}}$), a successive discrete sizing optimization at the fixed current n-th topology is performed. The process proceeds until a defined number (n_{fin}) of subsequent new topologies, which do

not fulfil the criterion $z_n^t < z_{OPT}$, is reached. The number n_{fin} is defined on the basis of the estimation of the non-convexity problem, when the objective is not improved strictly monotonically, and a new better solution is expected to be gained after some worse intermediate solutions. However, a small number (i.e., from two to five) of MINLP iterations, which do not yield an improvement in the objective, is generally sufficient to terminate the optimization process.

4.4.2. The Sequential Two-Phase (STP) MINLP Strategy

The Sequential Two-Phase (STP) MINLP (see Figure 4) strategy similarly to the MTP strategy consists of running a sequence of alternating topology optimization phases with continuous sizing variables and discrete sizing optimization phases (for better topologies only, $z_n^t < z_{OPT}$). The main difference between these two strategies is that the STP strategy starts with the initial phase ($n = 1$), where all alternative elements are active. The initial topology is thus the maximal topology. The process starts with the shape and continuous sizing optimization in the initial maximal topology, followed by the pre-screening of discrete dimensions. The subsequent discrete sizing optimization yields the first discrete solution with the value of the objective z_1^d. This solution is adopted as the currently best solution ($z_{OPT} = z_1^d$).

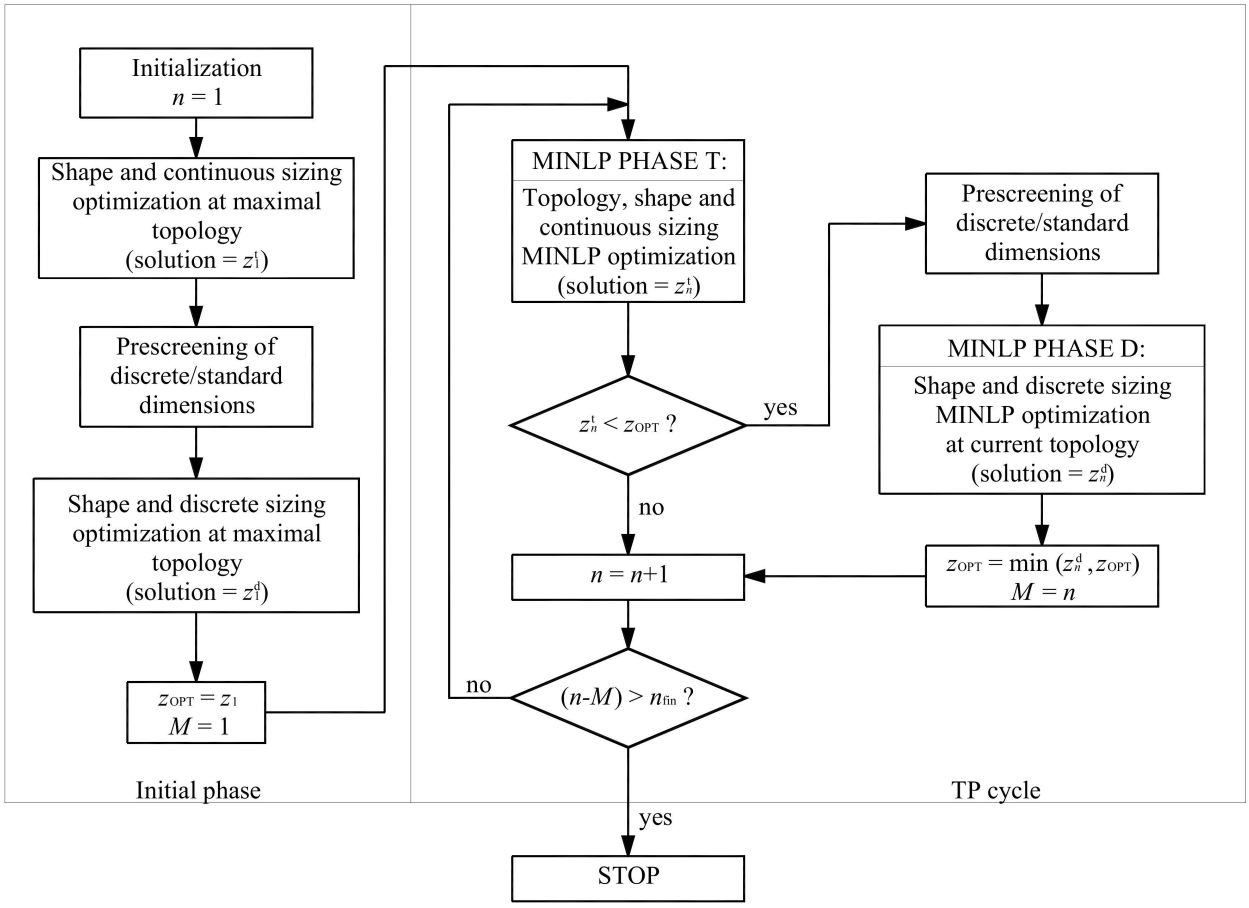

Figure 4. The Sequential Two-Phase MINLP strategy.

Further optimization cycles are then carried out identically according to MTP strategy, but without the deactivations of integer cuts. The discrete sizing variables are then relaxed into continuous parameters. The process proceeds ($n = n + 1$) with the topology and shape optimization searching for a topology that would yield a solution (value of the objective z_n^t) better than the currently best discrete solution, i.e., a solution which would satisfy the condition $z_n^t < z_{OPT}$. Only when the condition is satisfied is the subsequent discrete

sizing optimization at the fixed current topology performed, yielding the solution z_n^{d}. Two successive phases, i.e., the topology optimization and the discrete sizing optimization, together form the Two-Phase (TP) cycle. When the discrete solution z_n^{d} is obtained, the current TP cycle is concluded, and the next cycle begins. The process is terminated if a new topology satisfying the condition $z_n^{\mathrm{t}} < z_{\mathrm{OPT}}$ is not obtained in the defined number (n_{fin}) of successive MINLP iterations.

5. Numerical Example: Synthesis of a Ten-Bar Truss Cantilever

The MINLP topology, shape and discrete dimension optimization of a truss cantilever is presented as an illustrative example of truss synthesis. The ten-bar truss cantilever, see Figure 5, has frequently been used to test different optimization techniques on different optimization levels and, recently, has also been used for combined topology and discrete sizing optimization; see, for example, references [47–50].

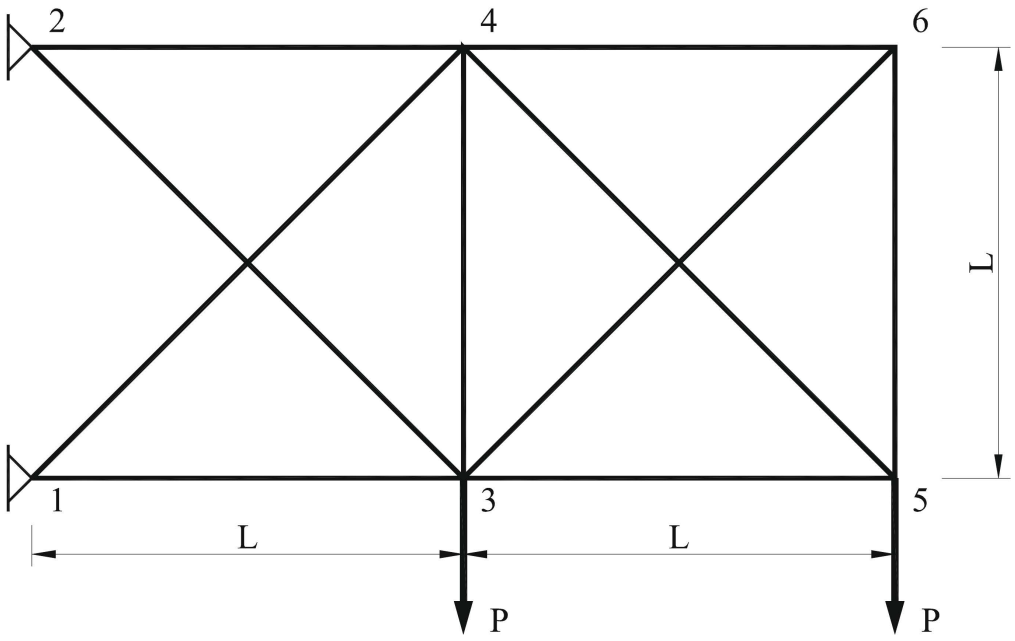

Figure 5. The ten-bar truss cantilever.

5.1. Input Data

The input data are taken from [49] and are as follows (see also Figure 5): L = 914.4 cm, P = 445.4 kN, Young's modulus E = 68.97 GPa, limit stresses $\sigma^{\mathrm{t,max}} = \sigma^{\mathrm{c,max}}$ = 172.4 MPa and the allowed vertical displacements of the unsupported joints $v_i^{\max}$ = 5.08 cm. The objective of the optimization is to minimize the weight of the structure. The term ρ in the objective function thus represents the unit weight of material 27126.4 N/m^3.

In the present example, the independent sizing variables are the cross-sectional areas of bars. A vector of l, $l \in L$ = {1,2,3, ... 16}, alternative discrete values for cross-sectional areas, is defined as follows:

$$\boldsymbol{q}_{i,j,l} = \{6.45, 19.35, 32.26, 51.61, 64.51, 67.74, 77.42, 96.77, 109.68, 141.94, 154.84, 167.74, 180.64, 187.10, 200.00, 225.81\}\ [\mathrm{cm}^2].$$

5.2. The Superstructure and Topological Alternatives

The truss cantilever is composed of 6 joints and 10 joint inter-connections—bars. The basis of the superstructure is composed from identical sets i and j, $i \in I$, $j \in J$, where

$I \equiv J$ = {1,2,3,4,5,6}. Regarding the defined bars in Figure 5, the inter-connection matrix **EL** is:

$$\mathbf{EL} = \left[el_{i,j}\right] = \begin{bmatrix} 0 & 0 & 1 & 1 & 0 & 0 \\ 0 & 0 & 1 & 1 & 0 & 0 \\ 0 & 0 & 0 & 1 & 1 & 1 \\ 0 & 0 & 0 & 0 & 1 & 1 \\ 0 & 0 & 0 & 0 & 0 & 1 \\ 0 & 0 & 0 & 0 & 0 & 0 \end{bmatrix}$$

Since each nodal load represents a separate load case, there are two load cases defined, $k \in K$ = {1,2}. According to the MINLP-TS formulation, the load vectors are defined as $\boldsymbol{p}_{\mathrm{x},1,i} \equiv \boldsymbol{p}_{\mathrm{x},2,i}$ = {0,0,0,0,0,0}, $\boldsymbol{p}_{\mathrm{y},1,i}$ = {0,0,−P,0,0,0} and $\boldsymbol{p}_{\mathrm{y},2,i}$ = {0,0,0,0,−P,0}. Joints 1 and 2 are supported in both X and Y directions; thus, the supporting vectors are $\boldsymbol{s}_{\mathrm{x},i} \equiv \boldsymbol{s}_{\mathrm{y},i}$ = {1,1,0,0,0,0}.

A single topological binary variable $y^{\mathrm{top}}_{i,i}$ is defined for each of the six joints ($y^{\mathrm{top}}_{1,1}$, $y^{\mathrm{top}}_{2,2}$, $y^{\mathrm{top}}_{3,3}$, $y^{\mathrm{top}}_{4,4}$, $y^{\mathrm{top}}_{5,5}$, $y^{\mathrm{top}}_{6,6}$), and a single topological binary variable $y^{\mathrm{top}}_{i,j}$ is subjected to each of the ten bars, i.e., to each pair of joints i and j, for which the inter-connection coefficient $el_{i,j} = 1$ ($y^{\mathrm{top}}_{1,3}$, $y^{\mathrm{top}}_{1,4}$, $y^{\mathrm{top}}_{2,3}$, $y^{\mathrm{top}}_{2,4}$, $y^{\mathrm{top}}_{3,4}$, $y^{\mathrm{top}}_{3,5}$, $y^{\mathrm{top}}_{3,6}$, $y^{\mathrm{top}}_{4,5}$, $y^{\mathrm{top}}_{4,6}$, $y^{\mathrm{top}}_{5,6}$). The remaining topological binary variables $y^{\mathrm{top}}_{i,j}$ are not active and are set to zero values. Binary variables are also defined for discrete sizing alternatives. Regarding the 16 different alternative discrete values from the defined vector $\boldsymbol{q}_{i,j,l}$, an extra binary variable $y^{\mathrm{st}}_{i,j,l}$ is defined for each l-th discrete value for each $i \rightarrow j$ bar. For the 10 defined bars, the considered problem thus involves 10 × 16 = 160 binary variables for discrete dimensions. In total, 6 + 10 + 160 = 176 binary variables are defined.

With respect to the supporting and loading of the structure as well as the arrangement of bars, joints 1 to 5 are fixed joints and will be included in all possible topology alternatives, while joint 6 is an alternative joint, since it may be included in or removed from the superstructure. In addition, bars 1→3, 3→5 and 2→4 are fixed bars, while all other bars represent alternative structural elements. Regarding the requirement for kinematical stability of the structure, a set of inter-connection logical constraints (18) for the present example can be written using Equations (18a–d) as follows:

$$y^{\mathrm{top}}_{1,4} + y^{\mathrm{top}}_{2,3} + y^{\mathrm{top}}_{3,4} - 2 \geq 0 \tag{18a}$$

$$y^{\mathrm{top}}_{3,6} + y^{\mathrm{top}}_{4,5} + y^{\mathrm{top}}_{5,6} - y^{\mathrm{top}}_{6,6} - 1 \geq 0 \tag{18b}$$

$$y^{\mathrm{top}}_{i,6} - y^{\mathrm{top}}_{6,6} \leq 0,\ i \in I,\ \forall\,(i,6) \ \Big|\ el_{i,6} = 1 \tag{18c}$$

$$y^{\mathrm{top}}_{4,6} - y^{\mathrm{top}}_{6,6} = 0 \tag{18d}$$

Equation (18a) concerns the panel 1–2–3–4 in which at least two bracing bars, i.e., one of the diagonals (1→4 or 2→3) and the vertical (3→4), or just both diagonals or all three of them have to be selected in order to provide the kinematical stability. The possible arrangements thus define four different topological alternatives for panel 1–2–3–4. In panel 3–4–5–6, joint 6 can be removed; therefore, according to Equation (18b), at least two bracing members have to be present when joint 6 is selected ($y^{\mathrm{top}}_{6,6}$ = 1), and a single bracing member is determined if joint 6 is rejected ($y^{\mathrm{top}}_{6,6}$ = 0). Equation (18c) calculates that all bars attached to joint 6 (i.e., bars 3→6, 4→6 and 5→6) will be rejected in the case when joint 6 is rejected, while bar 4→5 will be selected by the Equation (18b). Finally, bar 4→6 will always be selected if joint 6 is selected; see Equation (18d).

In the panel 3–4–5–6, 4 topological alternatives therefore exist when joint 6 is selected (equivalently to panel 1–2–3–4), plus one supplementary alternative when joint 6 is rejected, i.e., together, five different topological alternatives. The defined superstructure of the truss cantilever thus involves all the defined alternative combinations between the first and the second panel, i.e., 4 × 5 = 20 topological alternatives in total. The superstructure is schematically presented in Figure 6, where solid lines represent fixed structural elements

(joints and bars), while dashed lines denote alternative ones. It should be noted that eight topological binary variables are subjected to the defined eight fixed structural elements (five joints and three elements), while the other eight binary variables are attributed to the eight alternative structural elements. During the optimization, the values of the binary variables, which are subjected to the fixed elements, are fixed to 1. Thus, the total number of binary variables active in the optimization process is $176 - 8 = 168$.

It should be noted that in the case of seven alternative bars, the total number of all possible topological arrangements can be calculated as $2^7 = 128$. By including heuristics and by using simple logical inter-connection equations mentioned before, a considerable reduction of topological alternatives is made possible and, thus, also the combinatorial expanse of the problem.

The independent sizing variables are the cross-sectional areas of bars. Each cross-section area is defined by a single sizing design variable $d_{i,j}$, and the substituted function Equation (9) in the formulation MINLP-TS is simply $A_{i,j}^{\mathrm{sf}} = d_{i,j}$.

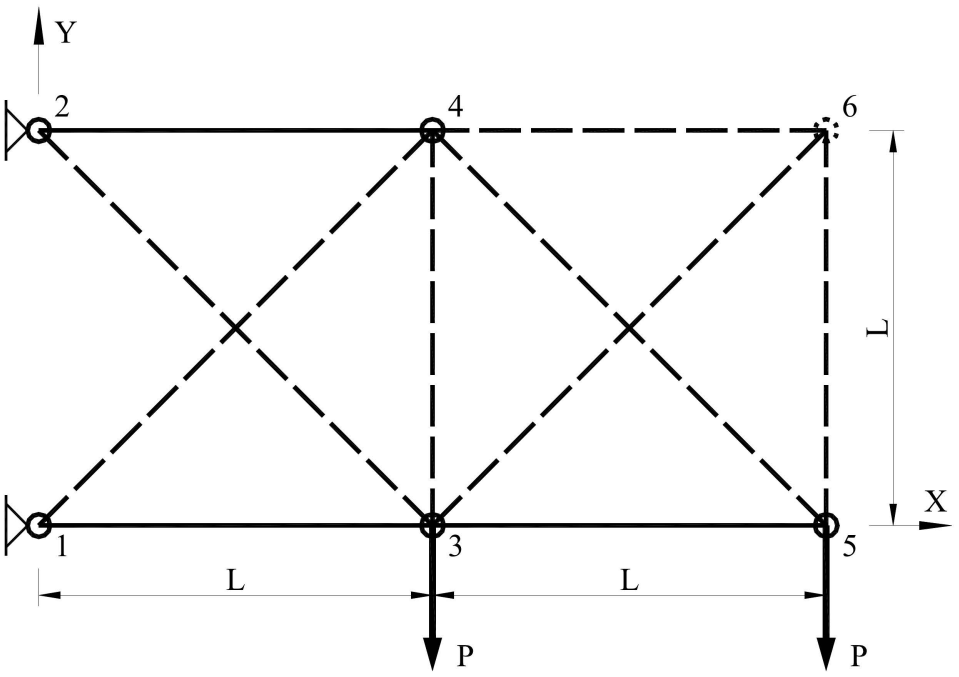

Figure 6. Fixed and alternative structural elements.

5.3. The MINLP Syntheses

Using the developed MINLP-TS formulation, the following examples of synthesis of the ten-bar truss cantilever were performed:

1. Example **TC10a**: *Topology and discrete dimension optimization without buckling constraints*. The structure is optimized at a fixed shape (at fixed nodal coordinates) under stress and displacement constraints, while the buckling constraints Equation (15) are excluded. The independent variables are the cross-sectional areas of bars $A_{i,j}$, with the lower/upper bounds defined to be equal to the smallest and the largest discrete value of vector $\boldsymbol{q}_{i,j,l}$ ($A_{i,j}^{\mathrm{ex,LO}} = 6.45$ cm^2, $A_{i,j}^{\mathrm{UP}} = 225.81$ cm^2).
2. Example **TC10b**: *Topology, shape and discrete dimension optimization without buckling constraints*. Alongside the sizing variables $A_{i,j}$, the joint coordinates ($^{\mathrm{c}}x_i$, $^{\mathrm{c}}y_i$), too, are now the independent variables. Considering the supporting and loading conditions, the coordinates of joints 4 and 6 are changeable, while the other joints are fixed. The bounds on shape variables are: $^{\mathrm{c}}x_4^{\mathrm{LO}} = 114$ cm, $^{\mathrm{c}}x_4^{\mathrm{UP}} = 1914$ cm, $^{\mathrm{c}}y_4^{\mathrm{LO}} = {}^{\mathrm{c}}y_6^{\mathrm{LO}} = 214$ cm, $^{\mathrm{c}}y_4^{\mathrm{UP}} = {}^{\mathrm{c}}y_6^{\mathrm{UP}} = 1214$ cm, $^{\mathrm{c}}x_6^{\mathrm{LO}} = 1028$ cm, $^{\mathrm{c}}x_6^{\mathrm{UP}} = 1928$ cm.

3. Example **TC10c**: *Topology and discrete dimension optimization including buckling constraints*. Buckling constraints Equation (15) are added to the example *TC10a*. The limit buckling stress of a compressed element is considered to be equal to the Euler buckling stress for circular cross-sections; thus, $\sigma_{i,j}^{cr} = A_{i,j}\pi E/(4 s_{i,j}^{sf\,2})$. The buckling lengths of elements are considered to be equal to the system lengths for both in-plane and out-of-plane buckling. Taking into consideration the buckling constraints, the cross-sectional areas of bars are expected to take higher values. The vector of discrete values is thus expanded to:

   $\boldsymbol{q}_{i,j,l}$= {6.45, 19.35, 32.26, 51.61, 64.51, 67.74, 77.42, 96.77, 109.68, 141.94, 154.84, 167.74, 180.64, 187.10, 200.00, 225.81, 245.14, 270.94, 290.30, 309.65, 322.55, 354.81, 387.06, 419.25} [cm^2].

   The new vector contains 24 alternative discrete values, and the total number of active binary variables is $10 \times 24 + 8 = 248$.
4. Example **TC10d**: *Topology, shape and discrete dimension optimization including buckling constraints*. The bounds on shape variables are the same as defined in example TC10b, while the buckling constraints and the vector of discrete cross-sectional areas are the same as in example TC10c.

All four examples of truss synthesis were carried out using both the MTP and the STP strategies in order to find and estimate the advantages of each MINLP strategy. In all the performed optimizations, the process was terminated after the theoretical result z_n^t of topology optimization with continuous sizing variables had not improved in five successive MINLP iterations; thus, $n_{fin} = 5$.

When pre-screening of binary variables for discrete dimensions was used, two neighboring (one lower and one upper) discrete values to the corresponding continuous value obtained in the previous continuous sizing optimization were active in the successive discrete sizing optimization. All other discrete values were temporarily deactivated, i.e., their associated binary variables were given zero value. The tests showed that in the case of discrete sizing optimization at fixed topology, the first feasible solution always represented the optimal result, while all following feasible solutions represented worse results. Thus, each discrete sizing optimization phase was concluded when the first feasible solution was obtained.

As an interface for mathematical modeling and data inputs/outputs GAMS (General Algebraic Modeling System) [81] was used. The syntheses were carried out by a user-friendly version of the MINLP computer package MIPSYN [78,82], the successor of PROSYN [4] and TOP [59–61]. MIPSYN is the implementation of many advanced optimization techniques, most important of which are the Modified OA/ER algorithm and multi-level MINLP strategies. GAMS/CONOPT [83] (generalized reduced gradient method) was used to solve NLP sub-problems, and GAMS/CPLEX [84] (Branch and Bound) was used to solve MILP master problems.

The convergences of the Modified OA/ER algorithm and the multi-level strategies applied to different examples of the synthesis of trusses are shown in Tables 1–4 for problems without buckling and in Tables A1–A4 in Appendix A for problems with buckling. Since the initial phase of the MTP strategy corresponds to topology optimization with continuous sizing variables, the convergences to the optimal topologies are also shown graphically in Figures 7 and 8 for problems without buckling and in Figures A1 and A2 in Appendix A for problems with buckling.

Table 1. Convergence of the Modified OA/ER algorithm and the **MTP** strategy, example **TC10a** (topology optimization, without buckling constraints).

Optimization Cycle	Optimization Phase	MINLP Iteration		Value of Objective Function (N)		No. of Active Bin. Var.	CPU Time (s)
		1	1. NLP	19,164.1340		-	0.102
		2	1. MILP	12,604.1900		8	0.030
			2. NLP	23,425.0739			0.090
		3	2. MILP	17,669.4100			0.030
	T		3. NLP	19,093.9919			0.070
		4	3. MILP	18,682.2600			0.040
$n = 1$			4. NLP	19,768.0154			0.117
		5	4. MILP	19,340.2000			0.040
			5. NLP	*19,010.8946*	(z^t)		0.102
		...	...	...		14	
	D	60	59. MILP	19,266.5400			
			60. NLP	***19,266.5406***	($z_{\mathbf{OPT}}$)		(*) 9.036
		61	60. MILP	12,627.5500		8	0.050
			61. NLP	23,425.0739			0.098
	T	62	61. MILP	15,732.7000			0.060
			62. NLP	19,768.0154			0.078
$n = 2$		63	62. MILP	15,826.6000			0.060
			63. NLP	19,093.9919	($z^t < z_{\mathrm{OPT}}$)		0.109
		...	...	...		12	
	D	90	89. MILP	19,559.6700			
			90. NLP	19,559.6663	($z^d > z_{\mathrm{OPT}}$)		(*) 5.320
		91	90. MILP	22,588.0650		8	0.070
			91. NLP	23,811.3197	($z_1{}^t > z_{\mathrm{OPT}}$)		0.078
		92	91. MILP	27,918.6900			0.110
			92. NLP	20,355.3448	($z_2{}^t > z_{\mathrm{OPT}}$)		0.090
		93	92. MILP	29,147.8200			0.100
$n = 3$	T		93. NLP	19,480.2377	($z_3{}^t > z_{\mathrm{OPT}}$)		0.152
		94	93. MILP	32,893.4400			0.110
			94. NLP	19,397.1404	($z_4{}^t > z_{\mathrm{OPT}}$)		0.148
		95	94. MILP	36,719.7900			0.200
			95. NLP	23,757.5489	($z_5{}^t > z_{\mathrm{OPT}}$)		0.160
							$\sum$ **= 16.650**

(*) sum of CPU times for the entire D phases; MINLP phase T: Topology and continuous sizing optimization; MINLP phase D: Discrete sizing optimization at fixed topology.

Table 2. Convergence of the Modified OA/ER algorithm and the **STP** strategy, example **TC10a** (topology optimization, without buckling constraints).

Optimization Cycle	Optimization Phase	MINLP Iteration		Value of Objective Function (N)		No. of Active Bin. Var.	CPU Time (s)
	T	1	1. NLP	19,164.1340	(z^t)	-	0.102
		...	...	...		20	
$n = 1$	D	39	38. MILP	19,492.8000			
			39. NLP	19,492.7981	(z_{OPT})		(*) 4.981
		40	39. MILP	12,208.5400		8	0.030
	T		40. NLP	23,425.0739			0.082
		41	40. MILP	15,354.2100			0.040
$n = 2$			41. NLP	19,093.9919	($z^t < z_{\mathrm{OPT}}$)		0.078
		...	...	...		12	
	D	68	67. MILP	19,559.6700			
			68. NLP	19,559.6663	(z_{OPT})		(*) 4.063

Table 2. *Cont.*

Optimization Cycle	Optimization Phase	MINLP Iteration	Value of Objective Function (N)			No. of Active Bin. Var.	CPU Time (s)
		69	68. MILP	15,589.9800		8	0.030
			69. NLP	19,768.0154			0.098
	T	70	69. MILP	16,178.2200			0.050
$n = 3$			70. NLP	19,010.8946	($z^t < z_{OPT}$)		0.133
		...	...	...			
	D	125	124. MILP	19,266.5400		14	
			125. NLP	***19,266.5406***	(**z_{OPT}**)		(*) 12.236
		126	125. MILP	16,999.0730		8	0.060
			126. NLP	23,811.3197	($z_1{}^t > z_{OPT}$)		0.082
		127	126. MILP	21,018.2310			0.140
			127. NLP	20,355.3448	($z_2{}^t > z_{OPT}$)		0.102
		128	127. MILP	22,321.5590			0.090
$n = 4$	T		128. NLP	19,480.2377	($z_3{}^t > z_{OPT}$)		0.102
		129	128. MILP	21,953.1130			0.130
			129. NLP	19,397.1404	($z_4{}^t > z_{OPT}$)		0.188
		130	129. MILP	23,778.8850			0.140
			130. NLP	23,757.5489	($z_5{}^t > z_{OPT}$)		0.191
							$\sum$ = 23.148

(*) sum of CPU times for the entire D phases; MINLP phase T: Topology and continuous sizing optimization; MINLP phase D: Discrete sizing optimization at fixed topology.

Table 3. Convergence of the Modified OA/ER algorithm and the **MTP** strategy, example **TC10b** (topology and shape optimization, without buckling constraints).

Optimization Cycle	Optimization Phase	MINLP Iteration	Value of Objective Function (N)			No. of Active Bin. Var.	CPU Time (s)
		1	1. NLP	17,025.3822		-	0.441
		2	1. MILP	13,466.9650		8	0.020
			2. NLP	17,919.2246			1.020
	T	3	2. MILP	16,313.8410			0.030
			3. NLP	17,346.7775			2.000
$n = 1$		4	3. MILP	17,148.3880			0.040
			4. NLP	*16,767.5972*	(z^t)		1.020
		...	...	...		16	
	D	11	10. MILP	15,609.8720			
			11. NLP	***16,936.2314***	(**z_{OPT}**)		(*) 9.380
		12	11. MILP	16,054.3400		8	0.040
			12. NLP	17,919.2246	($z_1{}^t > z_{OPT}$)		2.469
		13	12. MILP	17,259.0410			0.050
			13. NLP	17,346.7775	($z_2{}^t > z_{OPT}$)		0.492
		14	13. MILP	18,156.3480			0.060
$n = 2$	T		14. NLP	16,978.6881	($z_3{}^t > z_{OPT}$)		2.137
		15	14. MILP	22,324.8906			0.060
			15. NLP	19,004.3514	($z_4{}^t > z_{OPT}$)		0.449
		16	15. MILP	26,279.0820			0.080
			16. NLP	18,044.2047	($z_5{}^t > z_{OPT}$)		0.203
							$\sum$ = 19.991

(*) sum of CPU times for the entire D phases; MINLP phase T: Topology and continuous sizing optimization; MINLP phase D: Discrete sizing optimization at fixed topology.

Table 4. Convergence of the Modified OA/ER algorithm and the **STP** strategy, example **TC10b** (topology and shape optimization, without buckling constraints).

Optimization Cycle	Optimization Phase	MINLP Iteration	Value of Objective Function (N)			No. of Active Bin. Var.	CPU Time (s)
	T	1	1. NLP	17,025.3822	(z^t)	-	0.430
		...	...	...		20	
n = 1	D	8	7. MILP	15,967.6240			
			8. NLP	17,168.1830	(z_{OPT})		(*) 2.550
		9	8. MILP	13,466.9700		8	0.030
			9. NLP	17,919.2246			1.020
	T	10	9. MILP	16,313.8410			0.030
			10. NLP	17,346.7775			2.000
n = 2		11	10. MILP	17,148.3880			0.040
			11. NLP	16,767.5972	($z^t < z_{OPT}$)		1.031
		...	...	...		16	
	D	18	17. MILP	15,609.8720			
			18. NLP	***16,936.2314***	(**z_{OPT}**)		(*) 9.334
		19	18. MILP	19,935.8230		8	0.050
			19. NLP	16,978.6881	($z_1{}^t > z_{OPT}$)		2.160
		20	19. MILP	19,949.4000			0.051
			20. NLP	19,004.3514	($z_2{}^t > z_{OPT}$)		1.309
		21	20. MILP	21,562.9020			0.060
n = 3	T		21. NLP	18,044.2047	($z_3{}^t > z_{OPT}$)		0.199
		22	21. MILP	25,832.8800			0.070
			22. NLP	18,831.2099	($z_4{}^t > z_{OPT}$)		0.563
		23	22. MILP	28,257.8040			0.090
			23. NLP	17,898.1026	($z_5{}^t > z_{OPT}$)		0.461
							$\sum$ = 21.478

(*) sum of CPU times for the entire D phases; MINLP phase T: Topology and continuous sizing optimization; MINLP phase D: Discrete sizing optimization at fixed topology.

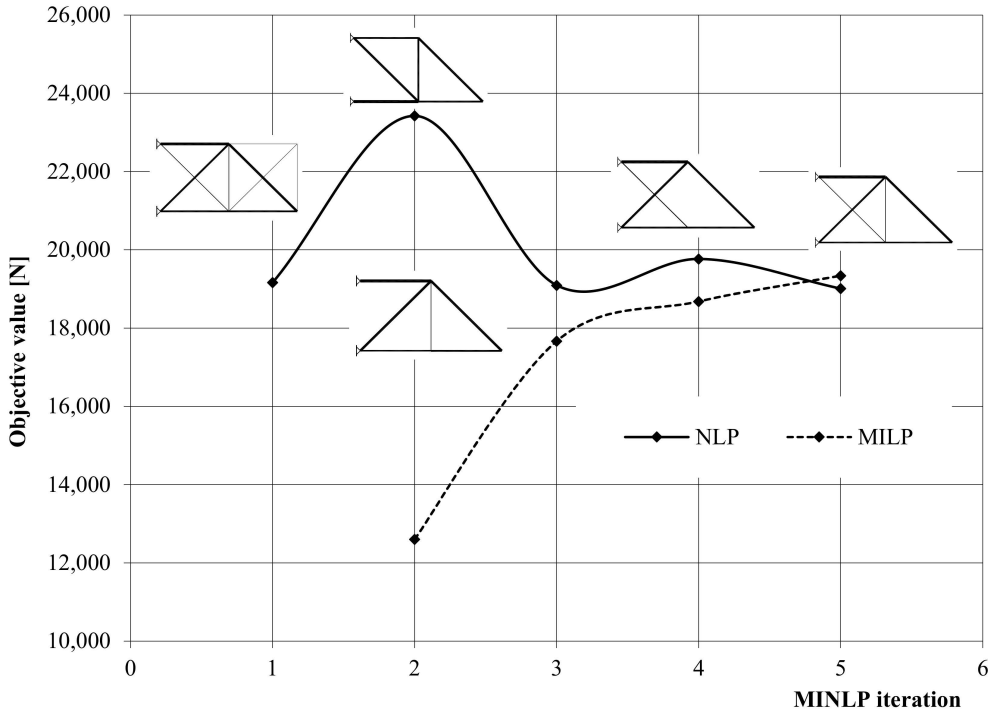

Figure 7. Convergence to the optimal topology, example TC10a (initial phase of the **MTP** strategy), example **TC10a** (topology optimization, without buckling constraints).

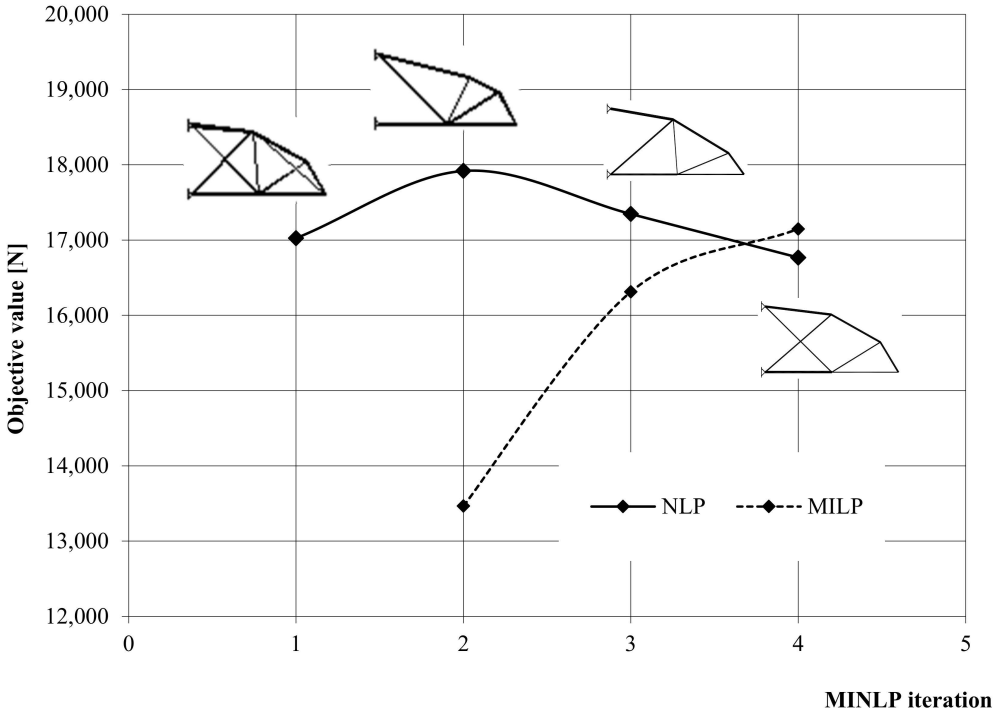

Figure 8. Convergence to the optimal topology (initial MINLP phase of the **MTP** strategy), example **TC10b** (topology and shape optimization, without buckling constraints).

5.4. Discussion of Results

The convergences of the performed truss syntheses illustrated in Tables 1–4 (without buckling) and Tables A1–A4 (with buckling) show that, in all four cases, the identical final/optimal result was obtained using both the MTP and STP MINLP strategies. Regarding the MTP strategy, the optimal result was always obtained after the first two optimization phases, i.e., after the topology optimization with continuous sizing variables followed by the discrete sizing optimization at the obtained fixed topology. Up to this point, the MTP strategy is identical to the original TP strategy [80], which is terminated after the first (and also final) solution with discrete sizing variables. The simple TP strategy would thus yield the same final results.

Table 5 illustrates and compares the MINLP iterations required and the CPU times for different synthesis examples performed by the discussed MINLP strategies.

Table 5. Comparison of optimization statistics for different MINLP strategies.

	MINLP Strategy	**Synthesis Example**			
		TC10a	**TC10b**	**TC10c**	**TC10d**
No. of MINLP iterations	TP	60	11	10	7
	MTP	95	16	21	13
	STP	130	23	21	35
CPU time (s)	TP	9.657	13.951	1.485	4.324
	MTP	16.650	19.991	3.537	10.889
	STP	23.148	21.478	3.344	43.806

The data captured in Table 5 show that the TP strategy required the lowest number of MINLP iterations as well as the lowest CPU times until the final/optimal result was attained in all four examples. With regard to the exposed outputs, the TP strategy proved to be the most effective from among all the compared MINLP strategies. However, as already mentioned, the TP strategy does not provide any information about the influence of discrete sizing variables on the possible change in topology. On the other hand, this

influence is accounted for both in the MTP as well as in the STP MINLP strategy. From among these two strategies, the MTP strategy proved to be the more convenient one.

It should be noted that the differences between the considered MINLP strategies become more expressed in cases when the NLP sub-problems become more extensive and difficult to solve. The CPU times of individual NLP sub-problems are considerably higher in examples TC10b and TC10d when compared to examples TC10a and TC10c. The former two examples include shape optimization. With the inclusion of shape variables (nodal coordinates), not only is the total number of variables higher but the problem is also more complex as the changing coordinates affect the calculation of internal forces (FE equations). In example TC10d, buckling constraints are also included. The inter-connection between buckling constraints and shape variables is additionally present, as the buckling resistance of a bar depends not only on its cross-sectional area but also on its buckling length. The CPU time of an individual NLP sub-problem in example TC10d is thus, on average, about 10 times higher than the CPU times of NLP sub-problems in example TC10a. Consequently, the differences between the applied MINLP strategies become more distinctive.

Although the STP strategy proved to be the least favorable strategy regarding both the number of MINLP iterations required as well as the CPU times spent, its advantage lies in the fact that more intermediate solutions are obtained. The first solution with discrete sizing variables is obtained at the initial topology with all alternative structural elements active. Considering these solutions, one can gain information about the influence of changeable topology in the final result with respect to different optimization constraints (with/without shape optimization and with/without buckling constraints). The optimal discrete sizing variables and continuous shape variables are therefore presented for both the initial and the optimal topologies of the four performed syntheses. The results are given in Tables 6 and 7 and graphically presented in Figures 9–12.

Table 6. Optimal results, examples without buckling constraints TC10a (topology optimization) and TC10b (topology and shape optimization).

	Example TC10a		**Example TC10b**	
	Initial Topology	**Optimal Topology**	**Initial Topology**	**Optimal Topology**
$A_{1,3}$ (cm^2)	96.77	96.77	141.94	141.94
$A_{1,4}$ (cm^2)	109.68	109.68	64.51	64.51
$A_{2,3}$ (cm^2)	19.35	19.35	51.61	51.61
$A_{2,4}$ (cm^2)	167.74	180.64	141.94	141.94
$A_{3,4}$ (cm^2)	19.35	19.35	6.45	-
$A_{3,5}$ (cm^2)	96.77	96.77	51.61	51.61
$A_{3,6}$ (cm^2)	6.45	-	51.61	51.61
$A_{4,5}$ (cm^2)	141.94	141.94	6.45	-
$A_{4,6}$ (cm^2)	6.45	-	109.68	109.68
$A_{5,6}$ (cm^2)	6.45	-	96.77	96.77
${}^{c}x_4$ (cm)			827.2361	909.1875
${}^{c}y_4$ (cm)			833.5299	801.3623
${}^{c}x_6$ (cm)			1566.7881	1580.4308
${}^{c}y_6$ (cm)			432.9369	417.6378
WEIGHT (N)	19,492.7981	**19,266.5406**	17,168.1830	**16,936.2314**

Table 7. Optimal results, examples with buckling constraints TC10c (topology optimization) and TC10d (topology and shape optimization).

	Example TC10c		**Example TC10d**	
	Initial Topology	**Optimal Topology**	**Initial Topology**	**Optimal Topology**
$A_{1,3}$ (cm^2)	387.06	387.06	387.06	387.06
$A_{1,4}$ (cm^2)	180.64	-	77.42	-
$A_{2,3}$ (cm^2)	109.68	109.68	51.61	51.61
$A_{2,4}$ (cm^2)	67.74	77.42	109.68	109.68
$A_{3,4}$ (cm^2)	6.45	270.94	6.45	154.84
$A_{3,5}$ (cm^2)	96.77	270.94	270.94	270.94
$A_{3,6}$ (cm^2)	419.25	-	167.74	-
$A_{4,5}$ (cm^2)	6.45	96.77	6.45	77.42
$A_{4,6}$ (cm^2)	64.51	-	96.77	-
$A_{5,6}$ (cm^2)	51.61	-	77.42	-
${}^{c}x_4$ (cm)			303.1833	1311.2365
${}^{c}y_4$ (cm)			829.4580	484.7189
${}^{c}x_6$ (cm)			1327.1457	-
${}^{c}y_6$ (cm)			486.3984	-
WEIGHT (N)	41,838.6690	**32,204.1317**	28,553.4737	**26,357.4575**

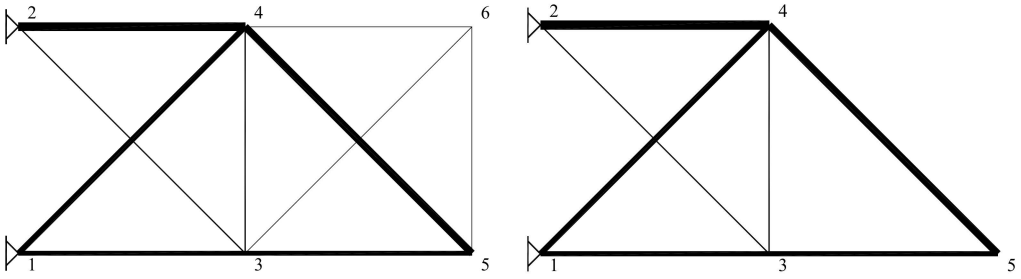

(**a**) (**b**)

Figure 9. Optimal solutions, example TC10a (topology optimization, without buckling constraints). (**a**) Initial topology; (**b**) optimal topology.

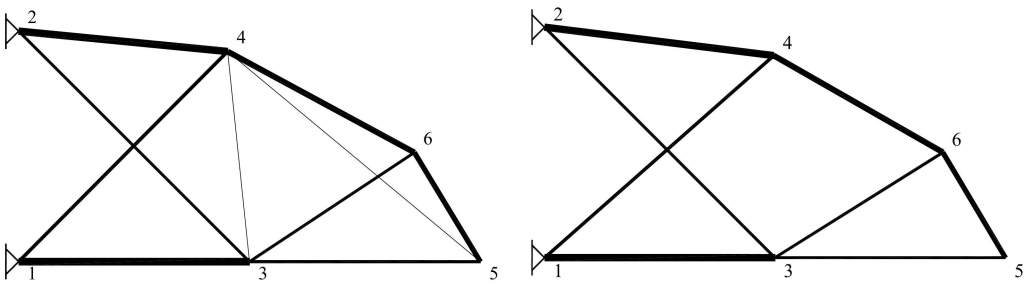

(**a**) (**b**)

Figure 10. Optimal solutions, example TC10b (topology and shape optimization, without buckling constraints). (**a**) Initial topology; (**b**) optimal topology.

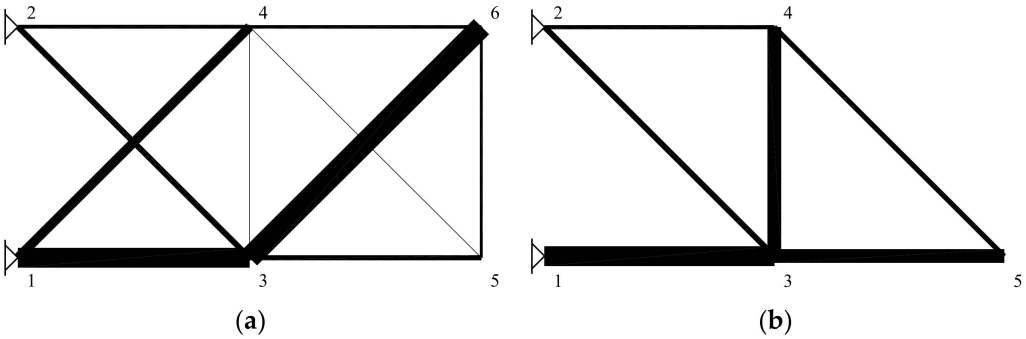

Figure 11. Optimal solutions, example TC10c (topology optimization, with buckling constraints). (**a**) Initial topology; (**b**) optimal topology.

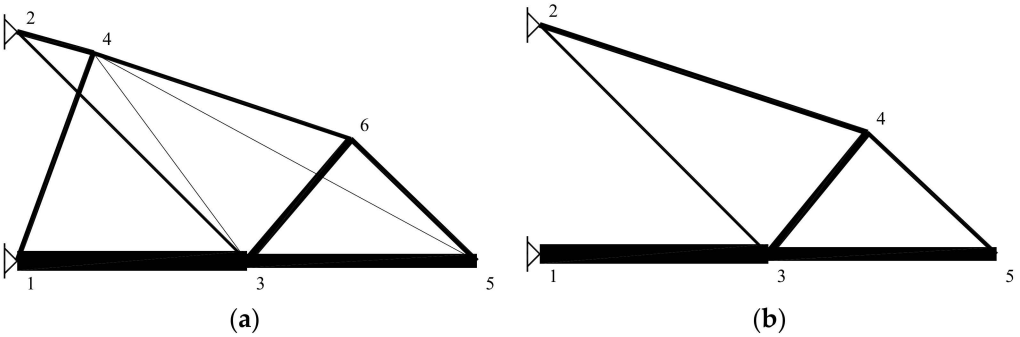

Figure 12. Optimal solutions, example TC10d (topology and shape optimization, with buckling constraints). (**a**) Initial topology; (**b**) optimal topology.

Table 6 comprises the results of the optimization without buckling constraints. The results of example TC10a can be regarded as the solutions of discrete sizing optimization at the fixed shape and topology (initial topology) and at fixed shape and changeable topology (optimal topology). Similarly, the results of example TC10b can be regarded as the solutions of the shape and discrete sizing optimization at the fixed topology (initial topology) and at the changeable topology (optimal topology). The results presented in Table 7 can be classified equivalently for the case of optimization with buckling constraints included. In this way, the achieved improvement in results at different optimization levels (topology and/or shape optimization) with regard to sizing optimization at fixed shape and topology (examples TC10a and TC10c at initial topology) can be estimated. The results of the comparative analysis are presented in Table 8.

Table 8. Improvement in final result (in %) at different optimization levels.

Buckling Constraints	Optimization Level		
	Shape	**Topology**	**Shape and Topology**
Not included	11.93	1.16	13.12
Included	31.75	23.03	37.00

In the case of optimization with stress and displacement constraints only (buckling is not included), surprisingly little decrease in optimal weight was achieved by the topology optimization. The shape optimization (at the fixed topology) yielded a considerably better result. However, when the buckling constraints were included, the topology optimization led to a considerably higher improvement, while shape optimization still yielded a better result. As expected in both cases, the best result was obtained by combining the topology and shape optimizations, yet it is obvious that almost a three times higher improvement in result (decrease in weight) was achieved when buckling constraints were included when

compared to the case of the optimization with stress and displacement constraints only (37.00% vs. 13.12%).

A more detailed analysis of the obtained results leads to a further finding. As has already been stated in the introductory sections, topology of truss structures was, in the past, often optimized by allowing very small (nonzero) lower bounds on cross-section areas of bars. When the cross-section areas of some bars were valued to the defined lower bounds, these bars were assumed to be redundant and were therefore excluded from the structure. Consequently, the optimal topology was adopted as the initial topology with the excluded »lower bound bars«.

When it comes to the results of the proposed MINLP truss synthesis, this assumption proves to be correct when the buckling constraints are excluded. The obtained optimal topologies in examples TC10a and TC10b are simply the initial topologies, where the bars with the lowest discrete cross-section area (6.45 cm^2) are excluded; see Table 6. This can be seen very clearly in Figures 9 and 10. On the other hand, when the buckling constraints are included, the discussed subject turns out to be different. In the optimal topologies of examples TC10c and TC10d, those bars are active, which, in the initial topology, took the lowest value. Excluding these bars would therefore lead to a non-optimal topology.

Beside stress, the buckling of compressed bars, is one of the basic conditions that has to be accounted for in the design process of a truss structure. In the initial topology, the compressed bars are subjected to buckling constraints and therefore require larger areas of cross-sections compared to tension bars, which are subjected to stress constraints only. The method of topology optimization with the elimination the least stressed bars mentioned above is thus not appropriate for real engineering structures.

Finally, the results of the proposed MINLP truss synthesis are compared to some results available in literature. The comparison of the optimal solution of example TC10a is presented in Table 9. The MINLP synthesis yielded the same result as the currently best solution presented in [49].

Table 9. Comparison of results.

	Reference [45]	**Reference [46]**	**Reference [47]**	**Reference [48]**	**Present Work**
$A_{1,3}$ (cm^2)	109.68	109.68	96.77	96.77	96.77
$A_{1,4}$ (cm^2)	96.77	109.68	109.68	109.68	109.68
$A_{2,3}$ (cm^2)	32.26	32.26	19.35	19.35	19.35
$A_{2,4}$ (cm^2)	167.74	167.74	167.74	180.64	180.64
$A_{3,4}$ (cm^2)	51.61	-	19.35	19.35	19.35
$A_{3,5}$ (cm^2)	96.77	77.42	109.68	96.77	96.77
$A_{3,6}$ (cm^2)	-	32.26	-	-	-
$A_{4,5}$ (cm^2)	141.94	109.68	141.94	141.94	141.94
$A_{4,6}$ (cm^2)	-	19.35	-	-	-
$A_{5,6}$ (cm^2)	-	19.35	-	-	-
WEIGHT (N)	20,058	19,712	19,266.7886	19,266.5406	19,266.5406

Additionally, all four examples of truss cantilever synthesis were performed using two commercial MINLP solvers, DICOPT [85] and BARON [86]. The previously discussed Two-Phase approach and the pre-screening of discrete sizing variables were applied in all cases.

DIPOCT also represents an implementation of the OA/ER algorithm. GAMS/CPLEX and GAMS/CONOPT were applied as the solvers for the MILP and NLP sub-problems, respectively. Two different stopping criteria were used:

1. Stop as soon as the bound defined by the objective of the MILP master problem is worse than the best NLP solution found (the same criterion as in the previous examples solved by MIPSYN), and
2. Stop as soon as the NLP sub-problems cease to improve.

Both criteria yielded the same final results.

By using BARON (Branch-And-Reduce Optimization Navigator), GAMS/CPLEX was applied as the LP solver, while GAMS/MINOS [87] was applied as the NLP solver. The maximum allowed CPU time of 10000 s was defined for each optimization phase, and multiple solutions were allowed.

The results obtained by different MINLP solvers are presented in Table 10. Compared to the solutions obtained by MIPSYN, DICOPT found the same solution in example TC10a, while in the remaining examples, worse solutions were found. BARON yielded the same solutions as MIPSYN in the examples TC10a and TC10c, while the remaining results (examples TC10b and TC10d) also represented worse solutions. In Table 11, the CPU times are also presented. For the solvers MISPYN and DICOPT, the CPU time until the termination of the Two-Phase procedure is shown. By using these two solvers, the CPU times are comparable, although DICOPT showed its advantages in the examples without buckling constraints (TC10a and TC10b), while MIPSYN proved to be more efficient in the remaining two examples. In the case of BARON, on the other hand, the optimization progress was much slower, and in most cases, the process continued to run until the CPU time limit of 10,000 s was reached. Therefore, the CPU times shown in Table 11 for the case of BARON represent the times spent until the best solutions (as shown in Table 10) were obtained.

Table 10. Results obtained by using different MINLP solvers.

Synthesis Example	MINLP (NLP/MILP, NLP/LP) Solver		
	DICOPT (CONOPT/CPLEX)	BARON (MINOS/CPLEX)	MIPSYN (CONOPT/CPLEX)
TC10a	19,266.5406	19,266.5406	19,266.5406
TC10b	17,078.4080	16,968.0110	16,936.2314
TC10c	32,590.3776	32,204.1317	32,204.1317
TC10d	26,516.4615	26,573.4506	26,357.4575

Table 11. The comparison of the CPU times (in seconds).

Synthesis Example	MINLP (NLP/MILP, NLP/LP) Solver		
	DICOPT (CONOPT/CPLEX)	BARON (MINOS/CPLEX)	MIPSYN (CONOPT/CPLEX)
TC10a	1.01	14.00	9.657
TC10b	1.00	2513.00	13.951
TC10c	3.67	8909.00	1.485
TC10d	16.24	6205.00	4.324

6. Conclusions

The present paper presents the Mixed-Integer Non-linear Programming (MINLP) approach to truss synthesis. The MINLP approach enables the topology, shape and discrete/standard cross-sectional dimensions to be optimized simultaneously. In the mixed continuous and discrete type of optimization problem, the continuous variables for continuous parameters (nodal coordinates, stresses, displacements) as well as the discrete binary variables for discrete decisions are defined. Binary 0–1 variables define the existence (1) or non-existence (0) of structural elements and are also subjected to the choice of the discrete/standard dimensions of cross-sections.

The proposed MINLP truss synthesis is performed through three steps. The first involves the generation of a truss superstructure of different topology and discrete dimension alternatives; the second presents the development of a special MINLP model formulation for truss superstructures (MINLP-TS); and the last contains a solution for the defined MINLP problem. The problems are solved by the Modified OA/ER algorithm.

Besides several non-linearities and non-convexities involved, the main difficulty of truss synthesis is that a very high number of discrete variables, particularly those associated with discrete/standard dimensions, may be included in the optimization. Multi-level MINLP strategies were thus developed and applied to make the solving of such comprehensive optimization problems possible. The main advantage of multi-level strategies is that the sub-set of binary variables, activated at each level, is considerably smaller than the full set. The additional reduction in the number of currently active binary variables for discrete dimensions was attained by the use of a special pre-screening procedure.

Two new types of multi-level strategies were presented, namely the Modified Two-Phase (MTP) and the Sequential Two-Phase (STP) MINLP strategies. Both strategies were developed on the basis of the classical Two-Phase (TP) strategy. The motive of developing new strategies was the fact that the TP strategy does not allow the topology to be changed after the discrete sizing optimization and therefore does not consider any interaction between topology and discrete sizing optimization levels. Out of the two new strategies, the MTP strategy proved to be the more convenient option regarding the MINLP iterations required and the CPU times spent. Considering the final/optimal result, however, the basic TP strategy proved also to be a useful tool for obtaining good solutions by spending short CPU times.

The proposed MINLP synthesis was applied to the simple and well-known numerical example of the ten-bar truss cantilever. The simultaneous topology and discrete sizing optimization was performed with/without the inclusion of shape optimization and with/without buckling constraints. The comparison of the obtained results with results available from literature proved the proposed MINLP synthesis to be a competitive optimization technique.

Some important conclusions regarding the buckling constraints of compressed bars also need to be emphasized. Not only do the buckling constraints represent a vital step of the design process, these constraints also have a crucial influence on the progress of topology optimization. When a truss is optimized, considering the stress and displacement constraints only, it is advisable for the low-stressed bars from the initial topology to be removed from the structure. By introducing buckling constraints, however, the lower stressed (mostly tensioned) bars from the initial topology are often a better choice for selection, while the higher stressed (mostly compressed) ones are rejected. Thus, it is not advisable to remove the low-stressed bars from the initial topology when the buckling constraints are considered. Rigorous topology such as that proposed in this paper should be employed to obtain optimal solutions. A considerably greater improvement in results (reduction in structural weight) was additionally achieved by the introduction of the shape optimization into the synthesis.

Author Contributions: Conceptualization, S.Š., Z.K. and S.K.; methodology, S.Š., Z.K. and S.K.; formal analysis, S.Š., Z.K. and S.K.; writing—original draft preparation, S.Š., Z.K. and S.K. All authors have read and agreed to the published version of the manuscript.

Funding: The authors acknowledge the financial support from the Slovenian Research Agency (grant numbers P2-0129 and P2-0032).

Institutional Review Board Statement: Not applicable.

Informed Consent Statement: Not applicable.

Data Availability Statement: The data presented in this study are available upon request from the corresponding author.

Conflicts of Interest: The authors declare no conflict of interest.

Appendix A

Table A1. Convergence of the Modified OA/ER algorithm and the **MTP** strategy, example **TC10c** (topology optimization, with buckling constraints).

Optimization Cycle	Optimization Phase	MINLP Iteration	Value of Objective Function (N)			No. of Active Bin. Var.	CPU Time (s)
$n = 1$	T	1	1. NLP	40,612.5684		-	0.180
		2	1. MILP	17,009.8900		8	0.030
			2. NLP	*31,376.7356*	(z^t)		0.148
		3	2. MILP	26,993.8600			0.031
			3. NLP	31,696.7121			0.172
		4	3. MILP	28,332.1100			0.050
			4. NLP	35,270.9973			0.121
		5	4. MILP	33,960.8800			0.050
			5. NLP	35,590.9738			0.109
	D	...	...	...		12	
		10	9. MILP	32,204.1300			
			10. NLP	***32,204.1317***	($z_{\mathbf{OPT}}$)		(*) 0.594
$n = 2$	T	11	10. MILP	32,483.5800		8	0.040
			11. NLP	31,696.7121	($z^t < z_{\mathrm{OPT}}$)		0.121
	D	...	...	...		14	
		16	15. MILP	32,524.1100			
			16. NLP	32,524.1082	($z^d > z_{\mathrm{OPT}}$)		(*) 0.832
$n = 3$	T	17	16. MILP	30,427.5500		8	0.050
			17. NLP	35,270.9973	($z_1{}^t > z_{\mathrm{OPT}}$)		0.148
		18	17. MILP	32,423.2100			0.060
			18. NLP	35,590.9738	($z_2{}^t > z_{\mathrm{OPT}}$)		0.082
		19	18. MILP	34,956.8920			0.080
			19. NLP	34,630.1695	($z_3{}^t > z_{\mathrm{OPT}}$)		0.082
		20	19. MILP	35,625.8000			0.081
			20. NLP	34,950.1460	($z_4{}^t > z_{\mathrm{OPT}}$)		0.117
		21	20. MILP	42,980.0600			0.090
			21. NLP	35,309.5418	($z_5{}^t > z_{\mathrm{OPT}}$)		0.109
							$\sum$ **= 3.537**

(*) sum of CPU times for the entire D phases; MINLP phase T: Topology and continuous sizing optimization; MINLP phase D: Discrete sizing optimization at fixed topology.

Table A2. Convergence of the Modified OA/ER algorithm and the **STP** strategy, example **TC10c** (topology optimization, with buckling constraints).

Optimization Cycle	Optimization Phase	MINLP Iteration	Value of Objective Function (N)			No. of Active Bin. Var.	CPU Time (s)
$n = 1$	T	1	1. NLP	40,612.5684	(z^t)	-	0.180
	D	...	...	...			
		4	3. MILP	41,838.6700			
			4. NLP	41,838.6690	(z_{OPT})		(*) 0.34
$n = 2$	T	5	4. MILP	17,009.8900		8	0.030
			5. NLP	31,376.7356	($z^t < z_{\mathrm{OPT}}$)		0.148
	D	...	...	...		12	
		10	9. MILP	32,204.1300			
			10. NLP	***32,204.1317***	($z_{\mathbf{OPT}}$)		(*) 0.594
$n = 3$	T	11	10. MILP	32,483.5800		8	0.040
			11. NLP	31,696.7121	($z^t < z_{\mathrm{OPT}}$)		0.121
	D	...	...	...		14	
		16	15. MILP	32,524.1100			
			16. NLP	32,524.1082	($z^d > z_{\mathrm{OPT}}$)		(*) 0.832

Table A2. *Cont.*

Optimization Cycle	Optimization Phase	MINLP Iteration	Value of Objective Function (N)			No. of Active Bin. Var.	CPU Time (s)
		17	16. MILP	30,427.5500		8	0.050
			17. NLP	35,270.9973	($z_1{}^t > z_{OPT}$)		0.148
		18	17. MILP	32,423.2100			0.060
			18. NLP	35,590.9738	($z_2{}^t > z_{OPT}$)		0.082
		19	18. MILP	34,956.8920			0.080
$n = 4$	T		19. NLP	34,630.1695	($z_3{}^t > z_{OPT}$)		0.082
		20	19. MILP	35,625.8000			0.081
			20. NLP	34,950.1460	($z_4{}^t > z_{OPT}$)		0.117
		21	20. MILP	42,980.0600			0.090
			21. NLP	35,309.5418	($z_5{}^t > z_{OPT}$)		0.109
							$\sum$ **= 3.344**

(*) sum of CPU times for the entire D phases; MINLP phase T: Topology and continuous sizing optimization; MINLP phase D: Discrete sizing optimization at fixed topology.

Table A3. Convergence of the Modified OA/ER algorithm and the **MTP** strategy, example **TC10d** (topology and shape optimization, with buckling constraints).

Optimization Cycle	Optimization Phase	MINLP Iteration	Value of Objective Function (N)			No. of Active Bin. Var.	CPU Time (s)
		1	1. NLP	27,755.0426		-	0.809
		2	1. MILP	16,094.2100		8	0.030
			2. NLP	31,189.2331			0.691
	T	3	2. MILP	22,727.4900			0.040
			3. NLP	*25,695.6485*	(z^t)		1.008
$n = 1$		4	3. MILP	26,774.4300			0.050
			4. NLP	38,672.9100			0.723
		...	...	...		12	
	D	7	6. MILP	25,695.6480			
			7. NLP	***26357.4575***	(z_{OPT})		(*) 0.973
		8	7. MILP	25,590.0000		8	0.060
			8. NLP	31,189.2331	($z_1{}^t > z_{OPT}$)		0.980
		9	8. MILP	28,733.3300			0.071
			9. NLP	29,436.0921	($z_2{}^t > z_{OPT}$)		0.531
		10	9. MILP	31,679.9400			0.070
			10. NLP	31,525.3188	($z_3{}^t > z_{OPT}$)		0.672
$n = 2$	T	11	10. MILP	31,679.9440			0.110
			11. NLP	[a] 23,004.7324			1.402
		12	11. MILP	32,453.3520			0.100
			12. NLP	30,543.6905	($z_4{}^t > z_{OPT}$)		1.211
		13	12. MILP	36,012.9370			0.100
			13. NLP	27,539.0495	($z_5{}^t > z_{OPT}$)		1.258
							$\sum$ **= 10.889**

(*) sum of CPU times for the entire D phases; [a] locally infeasible solution; MINLP phase T: Topology and continuous sizing optimization; MINLP phase D: Discrete sizing optimization at fixed topology.

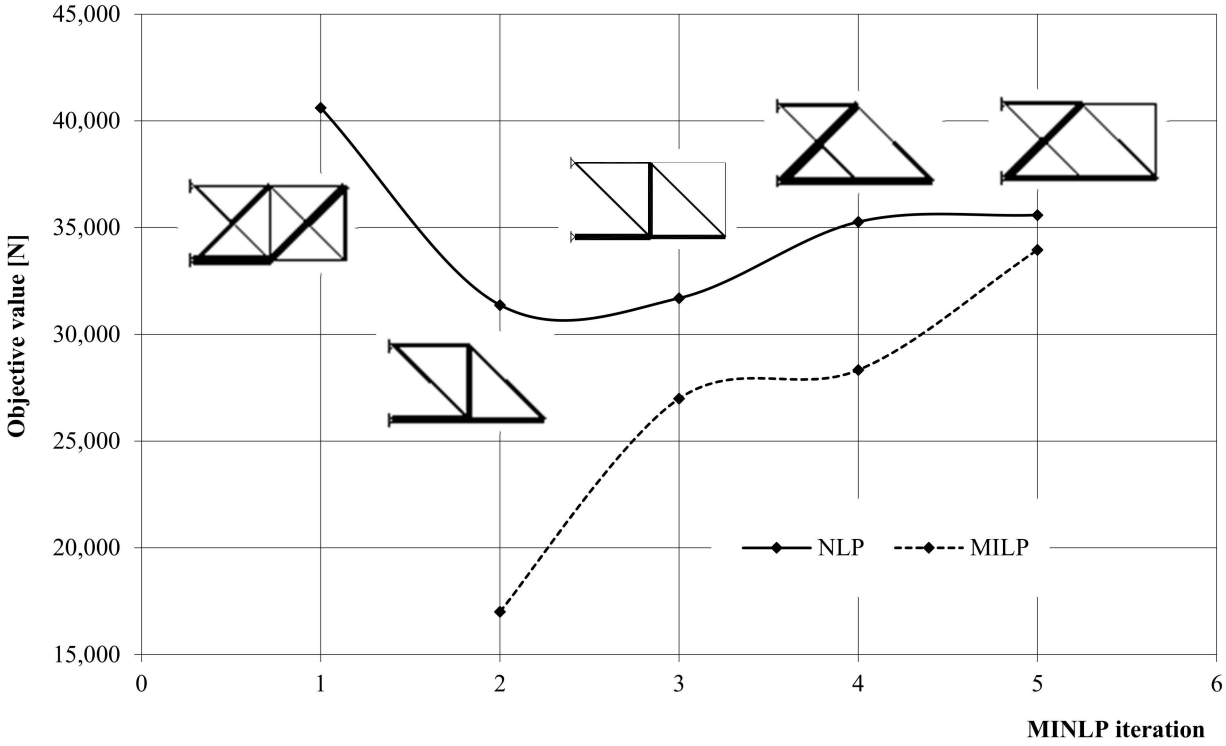

Figure A1. Convergence to the optimal topology (initial MINLP phase of the **MTP** strategy), example **TC10c** (topology optimization, with buckling constraints).

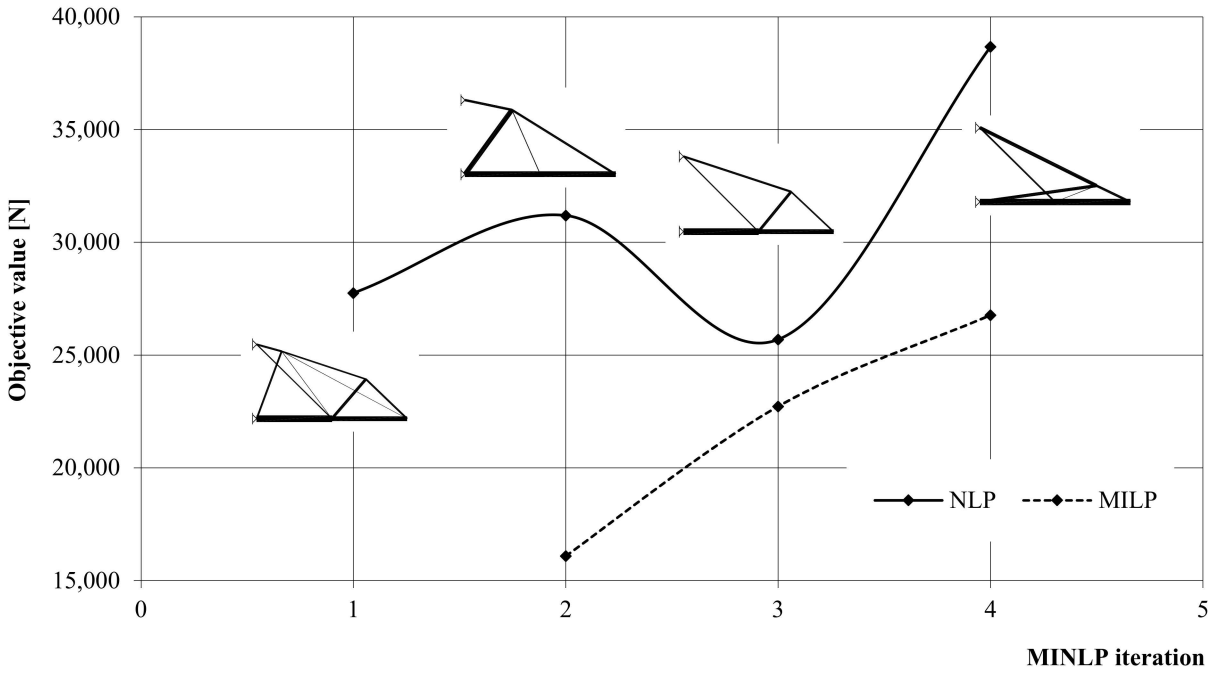

Figure A2. Convergence to the optimal topology (initial MINLP phase of the **MTP** strategy), example **TC10d** (topology and shape optimization, with buckling constraints).

Table A4. Convergence of the Modified OA/ER algorithm and the **STP** strategy, example **TC10d** (topology and shape optimization, with buckling constraints).

Optimization Cycle	Optimization Phase	MINLP Iteration	Value of Objective Function (N)			No. of Active Bin. Var.	CPU Time (s)
	T	1	1. NLP	27,755.0426	(z^t)	-	0.832
		...	...	...		20	
$n = 1$	D	10	9. MILP	26,036.1220			
			10. NLP	28,553.4737	(z_{OPT})		(*) 5.929
		11	10. MILP	16,234.9900		8	0.030
			11. NLP	31,189.2331			0.621
	T	12	11. MILP	18,417.8610			0.050
			12. NLP	29,436.0921			0.488
$n = 2$		13	12. MILP	20,849.8900			0.050
			13. NLP	25,695.6485	($z^t < z_{OPT}$)		0.898
		...	...	...		12	
	D	16	15. MILP	25,695.6480			
			16. NLP	***26,357.4575***	($\mathbf{z_{OPT}}$)		(*) 0.969
		17	16. MILP	25,275.5140		8	0.060
	T		17. NLP	38,672.9100			0.551
		18	17. MILP	26,827.2820			0.090
$n = 3$			18. NLP	25,948.8041	($z^t < z_{OPT}$)		12.102
	D	19	18. MILP	31,929.6360			0.090
			19. NLP	30,400.0000	($z^d > z_{OPT}$)		0.988
	T	20	19. MILP	27,143.8800		8	0.100
			20. NLP	25,794.2192	($z^t < z_{OPT}$)		0.891
$n = 4$		...	...	...		14	
	D	29	28. MILP	31,141.9100			
			29. NLP	28,847.4632	($z^d > z_{OPT}$)		(*) 8.336
		30	29. MILP	34,598.6040		8	0.120
			30. NLP	31,580.8787	($z_1{}^t > z_{OPT}$)		1.469
		31	30. MILP	30,636.5880			0.121
			31. NLP	29,643.5685	($z_2{}^t > z_{OPT}$)		3.168
		32	31. MILP	34,500.2680			0.170
			32. NLP	[a] 19,762.7370			0.309
$n = 5$	T	33	32. MILP	29,470.9030			0.140
			33. NLP	29,523.1464	($z_3{}^t > z_{OPT}$)		2.520
		34	33. MILP	23,966.5330			0.100
			34. NLP	28,227.8465	($z_4{}^t > z_{OPT}$)		1.199
		35	34. MILP	30,538.3790			0.180
			35. NLP	29,673.0156	($z_5{}^t > z_{OPT}$)		1.235
							$\sum$ = 43.806

(*) sum of CPU times for the entire D phases; MINLP phase T: Topology and continuous sizing optimization; MINLP phase D: Discrete sizing optimization at fixed topology.

References

1. Maxwell, J.C. On Reciprocal Figures, Frames and Diagrams of Forces. *Trans. R. Soc. Edinb.* **1869**, *26*, 1–40. [CrossRef]
2. Michell, A.G.M. The Limits of Economy in Frame Structures. *Philos. Mag.* **1904**, *8*, 589–597.
3. Schmit, L.A. Structural Design by Systematic Synthesis. In Proceedings of the 2nd Conference on Electronic Computations; ASCE: New York, NY, USA, 1960; pp. 105–122.
4. Kravanja, Z.; Grossmann, I.E. New developments and capabilities in PROSYN—An automated topology and parameter synthesizer. *Comput. Chem. Eng.* **1994**, *18*, 1097–1114. [CrossRef]
5. Dorn, W.S.; Gomory, R.E.; Greenberg, H. Automatic Design of Optimal Structures. *J. Mécanique* **1964**, *3*, 25–52.
6. Sved, G.; Ginos, Z. Structural Optimization Under Multiple Loading. *Int. J. Mech. Sci.* **1968**, *10*, 803–805. [CrossRef]
7. Sheu, C.Y.; Schmit, L.A. Minimum Weight Design of Elastic Redundant Trusses Under Multiple Static Loading Conditions. *AIAA J.* **1972**, *10*, 155–162. [CrossRef]
8. Kirsch, U.; Taye, S. On Optimal Topology of Grillage Structures. *Eng. Comput.* **1986**, *1*, 229–243. [CrossRef]

9. Kirsch, U.; Topping, B.H.V. Minimum Weight Designs of Structural Topologies. *J. Struct. Eng.* **1992**, *118*, 1770–1785. [CrossRef]
10. Sankaranarayanan, S.; Haftka, R.T.; Kapania, R.K. Truss topology optimization with simultaneous analysis and design. *AIAA J.* **1994**, *32*, 420–424. [CrossRef]
11. Achtziger, W. On simultaneous optimization of truss geometry and topology. *Struct. Multidiscip. Optim.* **2007**, *33*, 285–304. [CrossRef]
12. Goldberg, D.E. *Genetic Algorithms in Search, Optimization and Machine Learning*; Addison-Wesley: Reading, MA, USA, 1989.
13. Hajela, P.; Lee, E. Genetic Algorithms in Truss Topology Optimization. *Int. J. Solids Struct.* **1995**, *32*, 3341–3357. [CrossRef]
14. Rajan, S.D. Sizing, Shape and Topology Design Optimization of Trusses using Genetic Algorithm. *J. Struct. Eng.* **1995**, *121*, 1480–1487. [CrossRef]
15. Rajeev, S.; Krishnamoorthy, C.S. Genetic Algorithms Based Methodologies for Design Optimization of Trusses. *J. Struct. Eng.* **1997**, *123*, 350–358. [CrossRef]
16. Kawamura, H.; Ohmori, H.; Kito, N. Truss Topology Optimization by a Modified Genetic Algorithm. *Struct. Multidiscip. Optim.* **2002**, *23*, 467–472. [CrossRef]
17. Cagan, J.; Mitchell, W.J. Optimally Directed Shape Generation by Shape Annealing. *Environ. Plan.* **1993**, *20*, 5–12. [CrossRef]
18. Reddy, G.; Cagan, J. An Improved Shape Annealing Algorithm for Truss Topology Optimization. *J. Mech. Des.* **1995**, *117*, 315–321. [CrossRef]
19. Hasancebi, O.; Erbatur, F. Layout Optimisation of Trusses using Simulated Annealing. *Adv. Eng. Softw.* **2002**, *33*, 681–696. [CrossRef]
20. Sandgren, E. Multiple-objective, shape optimal design via genetic optimization. In *Computer Aided Optimium Design of Structures IV*; Hernandes, S., El-Sayed, M., Brebbia, C.A., Eds.; Computational mechanics publications: Southampton, UK; Boston, MA, USA, 1995; pp. 3–10.
21. Bennage, W.A.; Dhingra, A.K. Optimization of Truss Topology using Tabu Search. *Int. J. Numer. Methods Eng.* **1995**, *38*, 4035–4052. [CrossRef]
22. Bendsøe, M.P.; Kikuchi, N. Generating Optimal Topologies in Structural Design using a Homogenization Method. *Comput. Methods Appl. Mech. Eng.* **1988**, *71*, 197–224. [CrossRef]
23. Suzuki, K.; Kikuchi, N. A Homogenization Method for Shape and Topology Optimization. *Comput. Methods Appl. Mech. Eng.* **1991**, *93*, 291–318. [CrossRef]
24. Diaz, A.R.; Belding, B. On Optimum Truss Layout by a Homogenization Method. *J. Mech. Des.* **1993**, *115*, 367–373. [CrossRef]
25. Yildiz, A.R.; Öztürk, N.; Kaya, N.; Öztürk, F. Integrated Optimal Topology Design and Shape Optimization using Neural Networks. *Struct. Multidiscip. Optim.* **2003**, *25*, 251–260. [CrossRef]
26. Toakley, R. Optimum Design using Available Sections. *ASME J. Struct. Div.* **1968**, *94*, 1219–1241. [CrossRef]
27. Templeman, A.B.; Yates, D.F. A Linear Programming Approach to Discrete Optimum Design of Trusses. In *Optimization Methods in Structural Design*; Eschenauer, H., Olhoff, N., Eds.; BI Wissenschaftsverlag: Mannheim, Germany, 1983.
28. Zhou, D.M. An Improved Templeman's Algorithm for Optimum Design of Trusses with Discrete Member Sizes. *Eng. Optim.* **1986**, *9*, 303–312.
29. John, K.V.; Ramakrishnan, C.V. Minimum Weight Design of Trusses using Improved Move Limit of Sequential Linear Programming. *Int. J. Comput. Struct.* **1987**, *27*, 583–591. [CrossRef]
30. Bremicker, M.; Papalambros, P.Y.; Loh, H.T. Solution of Mixed-Discrete Structural Optimization Problems with a new Sequential Linearization Algorithm. *Comput. Struct.* **1990**, *37*, 451–461. [CrossRef]
31. Salajegeh, E.; Vaderplaats, G.N. Optimum Design of Trusses with Discrete Sizing and Shape Variables. *Struct. Optim.* **1993**, *6*, 79–85. [CrossRef]
32. Rajeev, S.; Krishnamoorthy, C.S. Discrete Optimization of Structures using Genetic Algorithms. *J. Struct. Eng.* **1992**, *118*, 1233–1250. [CrossRef]
33. Lin, C.Y.; Hajela, P. Genetic Algorithms in Optimization Problems with Discrete and Integer Design Variables. *Eng. Optim.* **1992**, *19*, 309–327. [CrossRef]
34. Erbatur, F.; Hasancebi, O.; Tütüncü, I.; Kilic, H. Optimal Design of Planar and Space Trusses with Genetic Algorithms. *Comput. Struct.* **2000**, *75*, 209–224. [CrossRef]
35. May, S.A.; Balling, R.J. A Filtered Simulated Annealing Strategy for 3D Optimization of Steel Frameworks. *Struct. Optim.* **1992**, *4*, 142–148. [CrossRef]
36. Pantelides, C.P.; Tzan, S.R. Optimal Design of Dynamically Constrained Structures. *Comput. Struct.* **1997**, *62*, 141–149. [CrossRef]
37. Cai, J.B.; Thiereut, G. Discrete Optimization of Structures using an Improved Penalty Function Method. *Eng. Optim.* **1993**, *21*, 293–306. [CrossRef]
38. Shih, C.J. Fuzzy and Improved Penalty Approaches for Multiobjective Mixed-Discrete Optimization in Structural Systems. *Comput. Struct.* **1997**, *6*, 559–565. [CrossRef]
39. Shih, C.J.; Yang, Y.C. Generalized Hopfield Network Based Structural Optimization using Sequential Unconstrained Minimization Technique with Additional Penalty Strategy. *Adv. Eng. Softw.* **2002**, *33*, 721–729. [CrossRef]
40. Jivotovski, G.A. Gradient Based Heuristic Algorithm and its Application to Discrete Optimization of Bar Structures. *Struct. Multidiscip. Optim.* **2000**, *19*, 237–248. [CrossRef]

41. Tong, W.H.; Liu, G.R. An Optimization Procedure for Truss Structures with Discrete Design Variables and Dynamic Constraints. *Comput. Struct.* **2001**, *79*, 155–162. [CrossRef]
42. Guerlement, G.; Targowski, R.; Gutkowski, W.; Zawidzka, J.; Zawidzki, J. Discrete Minimum Weight Design of Steel Structures using EC3 Code. *Strucural Multidiscip. Optim.* **2001**, *22*, 322–327. [CrossRef]
43. *Eurocode 3: Design of Steel Structures*; European Comitee for Standardization: Bruxelles, Belgium, 2005.
44. Bollapragada, S.; Ghattas, O.; Hooker, J.N. Optimal Design of Truss Structures by Logic-based Branch and Cut. *Oper. Res.* **2001**, *49*, 42–51. [CrossRef]
45. Ohsaki, M. Random Search Method based on Exact Reanalysis for Topology Optimization of Trusses with Discrete Cross-sectional Areas. *Comput. Struct.* **2001**, *79*, 673–679. [CrossRef]
46. Mela, K. Resolving issues with member buckling in truss topology optimization using a mixed variable approach. *Struct Multidisc Optim* **2014**, *50*, 1037–1049. [CrossRef]
47. Wang, Y.; Sun, H. The Topology Optimization of Structure with Discrete Variables under Multiload Case and Multiconstraint. *Acta Mech. Sin.* **1995**, *27*, 365–369.
48. Chai, S.; Shi, L.S.; Sun, H.C. An Application of Relative Difference Quotient Algorithm to Topology Optimization of Truss Structures with Discrete Variables. *Struct. Optim.* **1999**, *18*, 48–55. [CrossRef]
49. Kaveh, A.; Kalatjari, V. Topology Optimization of Trusses using Genetic Algorithm, Force Method and Graph Theory. *Int. J. Numer. Methods Eng.* **2003**, *58*, 771–791. [CrossRef]
50. Kaveh, A.; Shahrouzi, M. Simultaneous topology and size optimization of structures by genetic algorithm using minimal length chromosome. *Eng. Comput.* **2006**, *23*, 644–674. [CrossRef]
51. Kaveh, A.; Shojaee, S. Optimal design of skeletal structures using ant colony approach. *Int. J. Numer. Methods Eng.* **2007**, *70*, 563–581. [CrossRef]
52. Kaveh, A.; Shahrouzi, M. Optimal structural design family by genetic search and ant colony approach. *Eng. Comput.* **2008**, *25*, 268–288. [CrossRef]
53. Chen, S.Y.; Shui, X.F.; Li, D.F.; Huang, H. Improved genetic algorithm with two-level approximation for truss topology optimization. *Math. Probl. Eng.* **2015**, *2015*, 521482.
54. Kanno, J. Global optimization of trusses with constraints on number of different cross-sections: A mixed-integer second-order cone programming approach. *Comput Optim Appl* **2016**, *63*, 203–236. [CrossRef]
55. Mortazavi, A.; Togan, V. Simultaneous size, shape, and topology optimization of truss structures using integrated particle swarm optimizer. *Struct Multidisc Optim* **2016**, *54*, 715–736. [CrossRef]
56. Savsani, V.J.; Tejani, G.G.; Patel, V.K.; Savsani, P. Modified meta-heuristics using random mutation for truss topology optimization with static and dynamic constraints. *J. Comput. Des. Eng.* **2017**, *4*, 106–130. [CrossRef]
57. Degertekin, S.O.; Lamberti, L.; Ugur, I.B. Discrete sizing/layout/topology optimization of truss structures with an advanced Jaya algorithm. *Appl. Soft Comput.* **2019**, *79*, 363–390. [CrossRef]
58. Shahabsafa, M.; Fakhimi, R.; Lei, W.; He, S.; Martins, J.R.R.A.; Terlaky, T.; Zuluaga, L.F. Truss topology design and sizing optimization with guaranteedkinematic stability. *Struct. Multidisc. Optim.* **2021**, *63*, 21–38. [CrossRef]
59. Kravanja, S.; Kravanja, Z.; Bedenik, B.S. The MINLP approach to structural synthesis, Part I: A general view on simultaneous topology and parameter optimization. *Int. J. Numer. Methods Eng.* **1998**, *43*, 263–292. [CrossRef]
60. Kravanja, S.; Kravanja, Z.; Bedenik, B.S. The MINLP approach to structural synthesis, Part II: Simultaneous topology, parameter and standard dimension optimization by the use of the linked two-phase strategy. *Int. J. Numer. Methods Eng.* **1998**, *43*, 293–328. [CrossRef]
61. Kravanja, S.; Kravanja, Z.; Bedenik, B.S. The MINLP approach to structural synthesis, Part III: Synthesis of roller and sliding hydraulic steel gate structures. *Int. J. Numer. Methods Eng.* **1998**, *43*, 329–364. [CrossRef]
62. Kravanja, S. Optimization of the Sultartangi sliding gates in Iceland. *Int. J. Hydropower Dams* **2002**, *9*, 42–45.
63. Kravanja, S.; Turkalj, G.; Šilih, S.; Žula, T. Optimal design of single-story steel building structures based on parametric MINLP optimization. *J. Constr. Steel Res.* **2013**, *81*, 86–103. [CrossRef]
64. Kravanja, S.; Klanšek, U.; Žula, T. Mass, Direct Cost and Energy Life-Cycle Cost Optimization of Steel-Concrete Composite Floor Structures. *Appl. Sci.* **2021**, *11*, 10316. [CrossRef]
65. Šilih, S.; Kravanja, S.; Bedenik, B.S. *Finite Elements in Civil Engineering Applications: Proceedings of the Third Diana World Conference, Tokyo, Japan, 9–11 October 2002*; Hendriks, M.A.N., Rots, J.G., Eds.; Swets & Zeitlinger: Lisse, The Netherlands, 2002; pp. 369–373.
66. Kravanja, S.; Šilih, S. Optimization based comparison between composite I beams and composite trusses. *J. Constr. Steel Res.* **2003**, *59*, 609–625. [CrossRef]
67. Šilih, S.; Premrov, M.; Kravanja, S. Optimum design of plane timber trusses considering joint flexibility. *Eng. Struct.* **2005**, *27*, 145–154. [CrossRef]
68. Beale, E.M.L. Integer programming. In *The State of the Art in Numerical Analysis*; Jacobs, D., Ed.; Academic Press: London, UK, 1977; pp. 409–448.
69. Gupta, O.K.; Ravindran, A. A nonlinear mixed intefer programming and discrete optimization. In *Progress in Engineering Optimization*; Mayne, R.W., Ragsdell, K.M., Eds.; ASME: New York, NY, USA, 1984; pp. 295–520.
70. Quesada, I.; Grossmann, I.E. An LP/NLP based branch and bound algorithm for convex MINLP optimization problems. *Comput. Chem. Eng.* **1992**, *16*, 937–947. [CrossRef]

71. Westerlund, T.; Pettersson, F. An extended cutting plane method for solving convex MINLP problems. *Comput. Chem. Eng.* **1995**, *19*, 131–136. [CrossRef]
72. Benders, J.F. Partitioning procedures for solving mixed-variables programming problems. *Numer. Math.* **1962**, *4*, 238–252. [CrossRef]
73. Geoffrion, A.M. Generalized Benders decomposition. *J. Optim. Theory Appl.* **1972**, *10*, 237–260. [CrossRef]
74. Duran, M.A.; Grossmann, I.E. An Outer-Approximation Algorithm for a Class of Mixed-Integer Nonlinear Programms. *Math. Program.* **1986**, *36*, 307–339. [CrossRef]
75. Mawengkang, H.; Murtagh, B.A. Solving nonlinear integer programs with large-scale optimization software. *Annu. Opereatins Res.* **1986**, *5*, 425–437. [CrossRef]
76. Kocis, G.R.; Grossmann, I.E. Relaxation Strategy for the Structural Optimization of Process Flowsheets. *Inustrial Eng. Chem. Res.* **1987**, *26*, 1869–1880. [CrossRef]
77. Kravanja, S.; Bedenik, B.S.; Kravanja, Z. MINLP optimization of mechanical structures. In *Structural Optimization 93, The World Congress on Optimal Design of Structural Systems, Volume 1*; Herskovits, J., Ed.; Federal University of Rio de Janiero: Rio de Janeiro, Brasil, 1993; pp. 21–28.
78. Kravanja, S.; Soršak, A.; Kravanja, Z. Efficient multilevel MINLP strategies for solving large combinatorial problems in engineering. *Optim. Eng.* **2003**, *4*, 97–151. [CrossRef]
79. Kravanja, S.; Šilih, S.; Kravanja, Z. The multilevel MINLP optimization approach to structural synthesis: The simultaneous topology, material, standard and rounded dimension optimization. *Intern. J. Adv. Eng. Softw.* **2005**, *36*, 568–583. [CrossRef]
80. Kravanja, S.; Kravanja, Z.; Bedenik, B.S.; Faith, S. Simultaneous topology and parameter optimization of mechanical structures. In *Numerical Methods in Engineering 92, First European Conference on Numerical Methods in Engineering*; Hirsh, C., Zienkiewicz, O.C., Eds.; Elsevier: Amsterdam, The Netherlands, 1992; pp. 487–495.
81. Brooke, A.; Kendrick, D.; Meeraus, A. *GAMS (General Algebraic Modelling System), a User's Guide*; The Scientific Press: Redwood City, CA, USA, 1988.
82. Kravanja, Z. Challenges in sustainable integrated process synthesis and the capabilities of an MINLP process synthesizer MipSyn. *Comput. Chem. Eng* **2010**, *34*, 1831–1848. [CrossRef]
83. Drudd, A.S. CONOPT–A Large-Scale GRG Code. *ORSA J. Comput.* **1994**, *6*, 207–216. [CrossRef]
84. *GAMS/CPLEX User Notes*; ILOG Inc.: Geneva, Switzerland. Available online: https://www.gams.com/docs/pdf/cplexman.PDF (accessed on 2 December 2021).
85. Viswanathan, J.; Grossmann, I.E. A combined Penalty Function and Outer Approximation Method for MINLP Optimization. *Comput. Chem. Eng.* **1990**, *14*, 769–782. [CrossRef]
86. Sahnidis, N. BARON: A general purpose global optimization software package. *J. Glob. Optim.* **1996**, *8*, 201–205. [CrossRef]
87. Murtagh, B.A.; Saunders, M.A. *MINOS 5.1 User's Guide, Report SOL 83-20R*; Stanford University, Department of Operations Research: Stanford, CA, USA, 1987.